

# RSC Advances



This is an *Accepted Manuscript*, which has been through the Royal Society of Chemistry peer review process and has been accepted for publication.

*Accepted Manuscripts* are published online shortly after acceptance, before technical editing, formatting and proof reading. Using this free service, authors can make their results available to the community, in citable form, before we publish the edited article. This *Accepted Manuscript* will be replaced by the edited, formatted and paginated article as soon as this is available.

You can find more information about *Accepted Manuscripts* in the [Information for Authors](#).

Please note that technical editing may introduce minor changes to the text and/or graphics, which may alter content. The journal's standard [Terms & Conditions](#) and the [Ethical guidelines](#) still apply. In no event shall the Royal Society of Chemistry be held responsible for any errors or omissions in this *Accepted Manuscript* or any consequences arising from the use of any information it contains.

# Organometallic polymers for electrode decoration in sensing applications

Xueling Feng, Kaihuan Zhang, Mark A. Hempenius, and G. Julius Vancso\*

Materials Science and Technology of Polymers, MESA<sup>+</sup> Institute for Nanotechnology, University of Twente, 7500 AE Enschede, The Netherlands.

\* Correspondence to: Prof. G. Julius Vancso, Fax: +31 (0)53 489 3823; Tel: +31 53 489 2967, E-mail: [g.j.vancso@utwente.nl](mailto:g.j.vancso@utwente.nl).

## Abstract:

Macromolecules containing metals combine the processing advantages of polymers with the functionality offered by the metal centers. This review outlines the progress and recent developments in the area of electrochemical chemo/biosensors that are based on organometallic polymers. We focus on materials in which the metal centers provide function, allowing these materials to be used in electrochemical sensing applications based on various transduction mechanisms. Examples of chemo/biosensors featuring organometallic polymers that possess Fe, Os, Co and Ru are discussed.

## 1. Introduction

Organometallic polymers or metallopolymers refer to a wide range of metal-containing polymers, which have attracted rapidly expanding interest due to their unique chemical and physical properties and potential applications.<sup>1-9</sup> Different metallic centers in these substances can adopt various coordination numbers, oxidation states and different coordination geometries. Additionally, different chain geometries, degrees of polymerization, types of bonding (covalent or supramolecular) and variation of other parameters of the primary chemical structure provide access to new and versatile classes of functional materials.<sup>10</sup> The presence of metals in their main chain or side groups enables organometallic polymers to potentially play an unprecedented role in advanced technology in areas including nanoscale manufacturing,<sup>11-12</sup> ceramics precursors,<sup>13</sup> ferromagnetic materials,<sup>14</sup> separation, drug delivery,<sup>15</sup> molecular motors<sup>16</sup> and actuators,<sup>17</sup> photovoltaic devices,<sup>18</sup> catalysis,<sup>19</sup> sensing, energy conversion and storage, etc.

Interest in the development of new, easily processible materials that feature metal centers in synthetic polymer chains motivated scientists to tackle the synthesis of poly(vinylferrocene) by radical-polymerization.<sup>20</sup> Since this discovery, numerous synthetic approaches have been developed and adapted including polycondensation,<sup>21-22</sup> controlled radical polymerization, living ionic polymerization, ring-opening polymerization,<sup>23-25</sup> and electropolymerization<sup>26-27</sup> to form organometallic polymers that include main-chain or side-chain metal centers. Synthetic advances have also expanded from those that make use of traditional covalent bonds to incorporate metal centers in polymers, to approaches which use potentially reversible, “dynamic” binding by non-covalent coordination interactions that yield organometallic supramolecular polymers.<sup>1, 28</sup> Numerous reviews and monographs highlight and summarize the developments in the organometallic polymer field.<sup>25, 28-36</sup>

Stimulus responsive, or smart macromolecular materials which exhibit abrupt conformational and chemical changes in response to small variations of external stimuli, are of intense current interest.<sup>37-39</sup> The incorporation of metal centers in organometallic polymers offers many unique opportunities in the area of stimuli responsive materials. In most cases, organometallic polymers have intrinsic redox and luminescent properties inherited from the presence of metal centers and have been explored, e.g. as potential sensing materials, as they are capable of responding to external stimuli and by signals, which can be measured or recorded.<sup>40-41</sup>

Chemo/biosensors have been intensively researched due to their impact on numerous fields, such as in industrial processes, *in vitro* diagnostics (IVD), food quality control, chemical threat detection and environmental monitoring.<sup>42</sup> A chemo/biosensor is a device that detects the presence of particular chemical substances, a class of chemicals, or the occurrence of certain chemical reactions and biological cues qualitatively or quantitatively.<sup>40</sup> Chemo/biosensors have been developed for cations, anions, acids, vapors, volatile organics, biomolecules and for numerous other systems.<sup>42-44</sup> Usually, the sensor contains a receptor which can selectively respond to a particular analyte, or register chemical or biological changes; a transducer which converts this response into electrical (or other) signals and a processor which collects, amplifies, and provides a read-out of the signal.<sup>41</sup> Transducers include amperometric, potentiometric, gravimetric, piezoelectric, thermal or optical devices..

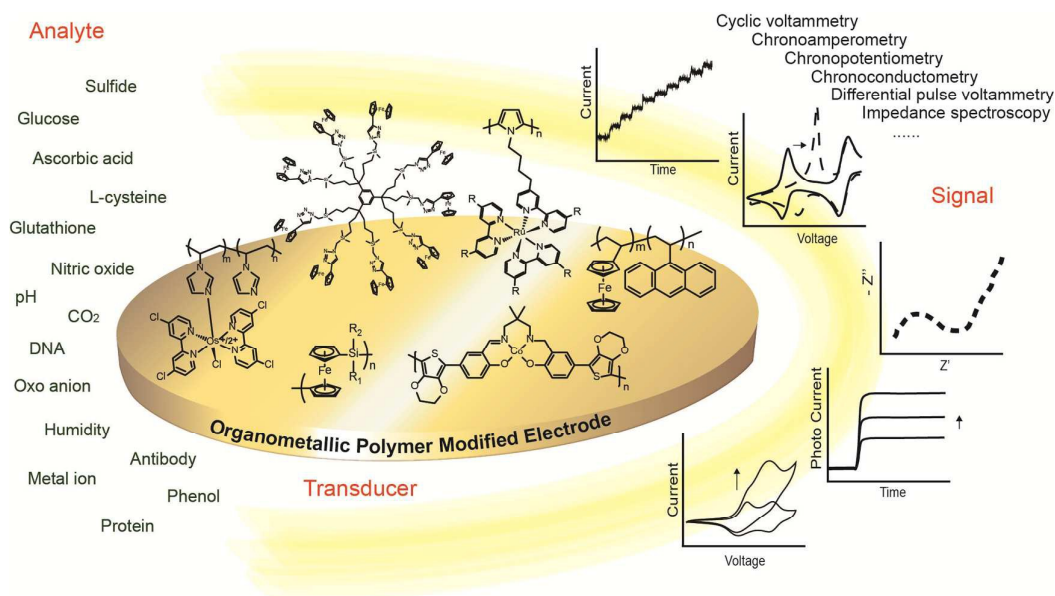


Figure 1. A schematic of electrochemical chemo/biosensors based on organometallic polymer modified electrodes.

Many commercial sensors have been developed based on inorganic-semiconductor or organic-polymeric films that react with the analyte molecules.<sup>42, 45</sup> The changes in chemical or physical properties of these films are monitored. Typically the concentration and chemical or physical characteristics of the analytes would determine the magnitude of the response. Although a variety of chemo/biosensors have been successfully commercialized, there is still a strong need for improvement in sensor fabrication with new materials and transduction mechanisms to enhance the sensing sensitivity, selectivity, reliability and robustness of the sensing process.

Owing to the intrinsic luminescent properties of some metals, organometallic polymers featuring such metallic centers have been widely used as luminescence sensors by monitoring the fluorescence or phosphorescence change of the sensing system due to the presence of analytes. Several reviews and articles discuss the development of luminescent chemo/biosensors based on organometallic polymers.<sup>9, 40, 46-50</sup> Organometallic polymers are also used as mechanical probes,<sup>51</sup> to fabricate sensitive membranes in surface acoustic wave devices for humidity sensing,<sup>52-55</sup> or in quartz crystal microbalance (QCM) devices to detect and quantify organic vapors.<sup>56</sup> Owing to the intrinsic redox and affinity properties of the metal, organometallic polymers have been employed in a variety of

electrochemical sensors by detecting the current, redox potential or resistance changes of the sensing system.

In this review, we survey the recent developments and highlight some milestones related to designing electrochemical chemo/biosensors with organometallic polymers.

## 2. Scope of organometallic polymers and metalorganic structures

Organometallic polymers can contain a variety of metal centers including main group (p-block) metals such as Sn and Pb,<sup>57</sup> transition metals such as Fe, Ir, Ru,<sup>47</sup> Cr, Os,<sup>58</sup> Pt,<sup>57</sup> Ag, Co,<sup>59</sup> or lanthanides and actinides such as Eu.<sup>2</sup> The position of the metal centers in the polymers and the nature of the linkages between them define the various structural types.<sup>1</sup> Based on the location of the metal centers, organometallic macromolecules can be divided into polymers with metal moieties embedded within the polymer backbone (Figure 2, polymer 1, 2.) and in the pendant side groups (Figure 2, polymer 3).<sup>59</sup> Considering the geometrical structure of macromolecules, the organometallic polymers may be linear (Figure 2, polymer 2), star-shaped (Figure 2, polymer 4) or dendritic (Figure 3).

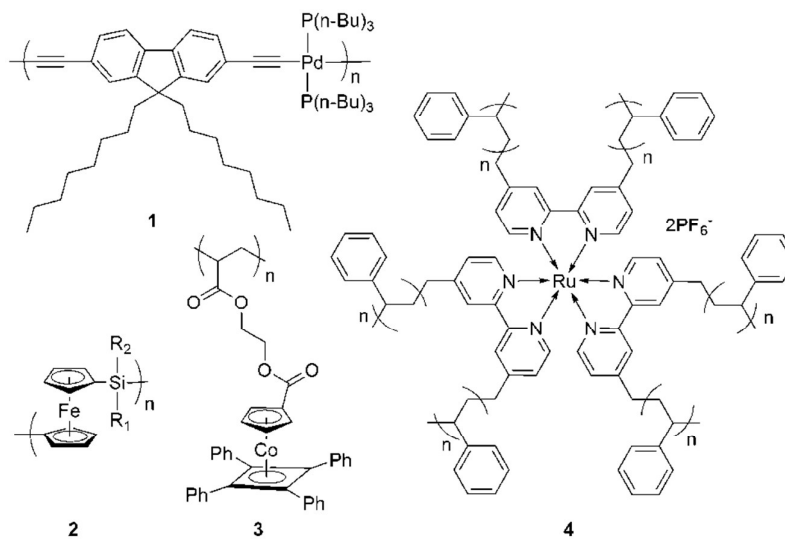


Figure 2. Examples of organometallic polymers. (1) Pd(II)-containing fluorene-based polymetallaynes,<sup>57</sup> (2) poly(ferrocenylsilanes),<sup>25</sup> (3) side chain Co(I) polymers featuring cyclopentadienyl-cobalt-cyclobutadiene (CpCoCb) units<sup>59</sup> and (4) Ru(II)-containing star-shaped polymer.<sup>60</sup>

The linkages binding the metals can be covalent, or non-covalent. Covalent linkages enable irreversible or “static” binding of the metal while non-covalent coordination can allow potentially reversible “dynamic” binding, forming organometallic supramolecular polymers (Figure 4).<sup>1</sup> Metal-organic frameworks (MOFs), consisting of metal ions coordinated to organic molecules, are special organometallic polymers which represent an interesting class of crystalline molecular materials synthesized by combining metal-connecting points and bridging ligands with one-, two-, or three-dimensional structures.<sup>61</sup>

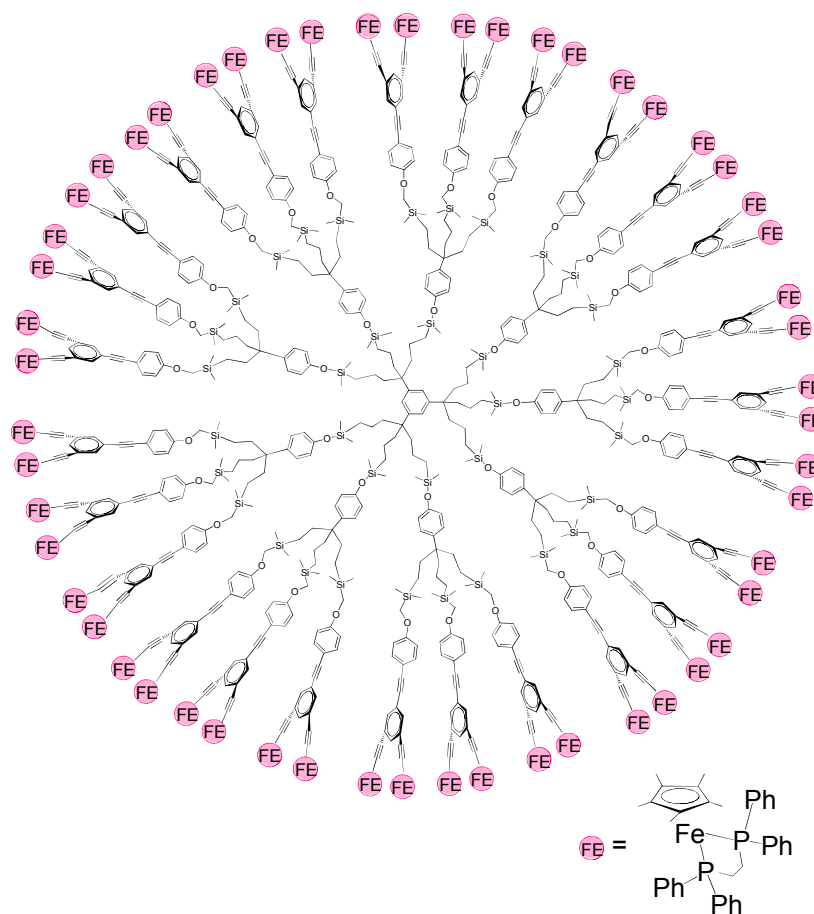


Figure 3. Dendrimer with redox-active  $\text{Cp}^*\text{Fe}^{\text{II}}(\text{dpppe})$ -alkynyl centers ( $\text{Cp}^* = \eta^5\text{-C}_5\text{Me}_5$ ,  $\text{dpppe} = 1,2$ -bis(diphenylphosphino) ethane).<sup>62</sup>

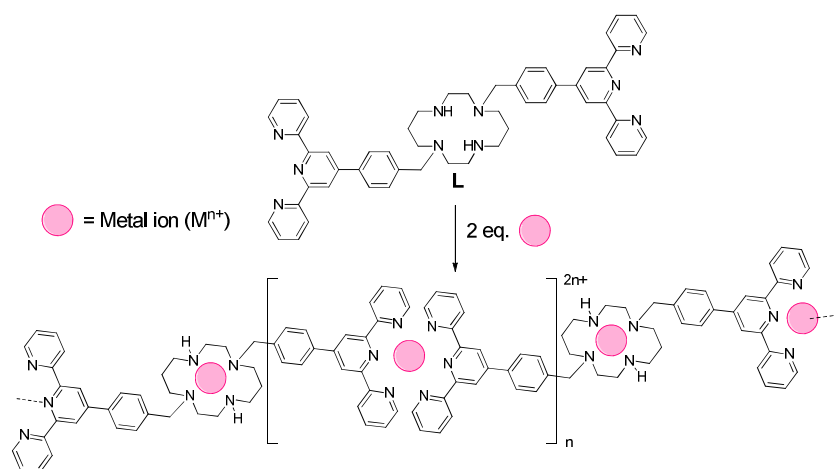


Figure 4. Organometallic polymer obtained by “dynamic binding” using  $M^{2+}$  complexation by the tritopic bis-terpyridine cyclam ligand.<sup>63</sup> Reprinted with permission from *ref. 63*. Copyright (2013) Elsevier Inc.

### 3 Electrochemical sensors

Electrochemical chemo/biosensors should possess high selectivity, excellent sensitivity, low cost, ease of use, portability and simplicity of construction.<sup>64</sup> The analytes and reactions being monitored by electrochemical methods typically cause a measurable current (amperometry), a measurable charge accumulation or potential (potentiometry), or alter the conductive properties of the medium between electrodes (conductometry).<sup>41</sup> Many signal transduction schemes require a physical interface which generally involves chemically modified electrodes<sup>65</sup> to tune electrochemical responses to analytes and improve detection sensitivity, selectivity and device stability. When preparing chemically modified electrodes, a thin film with a particular chemical composition and certain architecture is usually coated onto, or chemically bound to, the electrode surface in a rationally designed way, providing the desired properties to the electrode.<sup>66</sup>

Major basic designs of thin polymer films include end-tethered polymer chains, films from functional particles, electrostatic layer-by-layer assembled films,<sup>67</sup> block-copolymer films, crosslinked thin polymer or hydrogel thin films, porous films, etc.<sup>68-70</sup> The techniques involved to obtain these films include drop-casting and spin-coating, inkjet printing, doctor blading, layer-by-layer assembly, grafting to and from methods, electropolymerization, etc.<sup>71-73</sup>

Electrodes, modified with organometallic polymers, possess many interesting features that can be exploited for electroanalytical and sensor applications. The properties of the electrode and its sensing ability are easily controlled by carefully choosing the proper metal, the ligands and the decoration architectures. For example, by adapting the ligands to a certain metal (e.g. iron, cobalt), the redox properties can be tuned as the standard electrode potential is influenced by the ligands (Table 1). Additionally, organometallic polymer decorated electrodes often have a large surface with high redox-active center loadings.

Table 1. Standard electrode potentials of common half-reactions in aqueous solution, measured relative to the standard hydrogen electrode at 25 °C with all species at unit activity.<sup>74</sup>

Half-reactions	$E^0 / \text{V}$
$\text{Fe}^{3+} + \text{e}^- \rightarrow \text{Fe}^{2+}$	+0.77
$\text{Fe}(\text{phen})_3^{3+} + \text{e}^- \rightarrow \text{Fe}(\text{phen})_3^{2+}$	+1.13
$\text{Fe}(\text{CN})_6^{3-} + \text{e}^- \rightarrow \text{Fe}(\text{CN})_6^{4-}$	+0.36
$[\text{Ferrocenium}]^+ + \text{e}^- \rightarrow \text{Ferrocene}$	+0.40
$\text{Co}^{3+} + \text{e}^- \rightarrow \text{Co}^{2+}$	+1.92
$\text{Co}(\text{NH}_3)_6^{3+} + \text{e}^- \rightarrow \text{Co}(\text{NH}_3)_6^{2+}$	+0.06
$\text{Co}(\text{phen})_3^{3+} + \text{e}^- \rightarrow \text{Co}(\text{phen})_3^{2+}$	+0.33
$\text{Co}(\text{C}_2\text{O}_4)_3^{3-} + \text{e}^- \rightarrow \text{Co}(\text{C}_2\text{O}_4)_3^{4-}$	+0.57

### 3.1 Sensors based on ferrocene-containing organometallic polymers

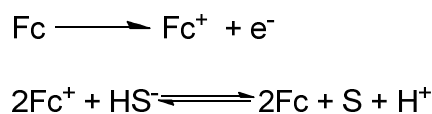
Metallocenes exhibit remarkable electronic and optical properties which make them versatile building blocks for incorporation into polymer systems. Ferrocene (Fc) and its derivatives represent the most common metallocenes applied in organometallic polymers. Discovered in 1951,<sup>75</sup> ferrocene has a “sandwich” like structure with two cyclopentadienyl (Cp) rings coordinated to one Fe(II) cation as a neutral complex. The complex is small with dimensions of 4.1 Å × 3.3 Å, while the ferrocenium ion, the oxidized form of ferrocene, has dimensions of 4.1 Å × 3.5 Å.<sup>76</sup> Considering the steric requirements,



van der Waals radii have been recommended for indicating the molecular dimensions.<sup>77</sup> Thus, the neural species is ca. 6.7 Å long along the cylinder axis and ca. 5.7 Å wide.<sup>78</sup> The dimensions of the ferrocenium ion are only slightly larger (cylinder axis of ca 6.8 Å, diameter ca. 5.9 Å). Because of the favorable electrochemical characteristics, such as low oxidation potential (pH-independent), fast electron-transfer rate, high levels of stability in its two redox states, low cost, and well-defined synthetic procedures for many derivatives, ferrocene has proved to be an effective building block in electrocatalysis and electrochemical sensing materials.<sup>79-80</sup>

### 3.1.1 Polymers with ferrocene side groups

As mentioned, organometallic polymers with metals in side groups are often utilized in electrochemical sensing. For example, the organometallic polymer poly(vinylanthracene-*co*-vinylferrocene), containing pendent ferrocene groups, was synthesized to form a dual pH/sulfide electrochemical sensor.<sup>81</sup> The electrode decoration was conducted by abrasively immobilizing the organometallic polymer onto the surface of polished basal plane pyrolytic graphite (BPPG) electrode by gently rubbing the material onto the electrode surface. The oxidation of the ferrocene moiety involves an electrocatalytic reaction with sulfide (Scheme 1), showing an enhancement in the oxidative peak current: the ferrocene moiety is oxidized at the electrode surface while the sulfide reduces the ferrocenium ion back to ferrocene, which is then re-oxidized at the electrode surface. The current increased linearly with the sulfide concentration over the range of 0.2-2 mM at pH values above 6.9 (Figure 5A). By monitoring the current changes, sulfides could be electrochemically detected by the poly(vinylanthracene-*co*-vinylferrocene) decorated electrodes.



Scheme 1. The electrocatalytic reaction of sulfide with ferrocene moieties in a pH/sulfide electrochemical sensor.<sup>81</sup>

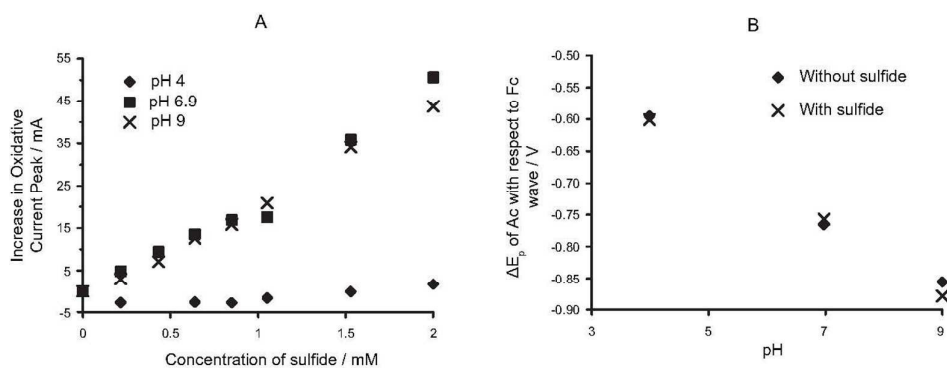


Figure 5. A) Dual pH/sulfide electrochemical sensor. Calibration plot of the normalized peak current of the ferrocene vs. sulfide concentration, at various pH values. B) Calibration plot of the variation in the peak potential of the anthracene units with respect to the ferrocene units, as a function of pH.<sup>81</sup> Reprinted with permission from *ref. 81*. Copyright (2006) Wiley-VCH.

Electrodes covered with this organometallic polymer are also pH sensitive. The two-electron oxidation potential of the anthracene moiety was linearly related to the pH value (Figure 5B), and followed a Nernstian response with the protons, while the redox-active but pH-insensitive ferrocene moiety acts as the reference species (Figure 6). Additionally, the pH response was found to be temperature independent, showing an insignificant variation (<10 mV) over a range of temperatures. The ferrocene units here had a dual role, as an internal calibrating agent for the system and as an electrocatalyst involved in the sensing mechanism. Owing to the support of the polymer chain, the signal of the ferrocene group in this organometallic polymer at elevated temperatures showed a superior stability compared to that of ferrocene in solutions.<sup>82</sup>

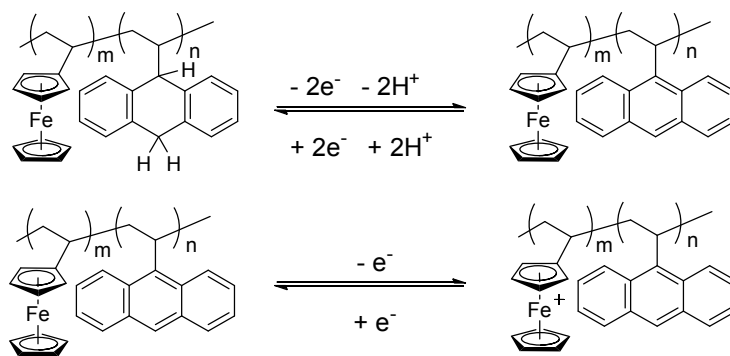


Figure 6. The proposed electrochemical pathway for anthracene and ferrocene moieties in a pH/sulfide electrochemical sensor.<sup>81</sup>

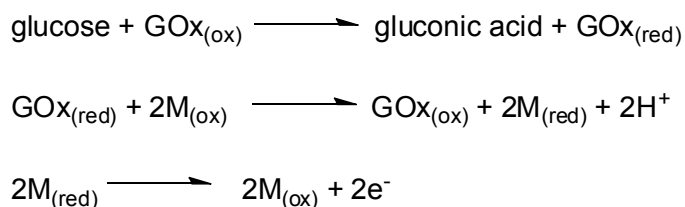
Using similar organometallic polymers, the pH sensing ability was enhanced by associating the polymers with carbon nanotubes (CNTs).<sup>83</sup> In such systems the plot of the anthracene moiety peak potential against pH was linear up to at least pH 11.6, showing a wider pH sensing range.

Zhang et al. reported the fabrication of cationic poly(allylamine)ferrocene grafts on the surface of a gold electrode modified with negatively charged alkanethiols by electrostatic interaction.<sup>84</sup> The modified electrode was used as an ascorbic acid sensor. The cyclic voltammogram of the decorated electrode showed, upon addition of ascorbic acid, an increase of the catalytic current and a decrease of the overpotential of ascorbic acid, which provides evidence for excellent electrocatalytic performance of the ferrocene-containing polymer in ascorbic acid oxidation. The modified electrode has many advantages as it is simple to fabricate, has a fast response and good chemical and mechanical stability.

Organometallic polymers containing ferrocene moieties have also been designed and synthesized to construct amperometric biosensors with enzymes in which the Fc moieties act as mediators to enable the shuttling of electrons between the enzymes and the electrode.<sup>85</sup> In most cases, the electrode surfaces were prepared by drop casting using mixtures of organometallic polymers and enzymes. Examples of redox ferrocene-containing organometallic polymers used in enzymatic sensing include poly(vinylferrocene-*co*-hydroxyethyl methacrylate),<sup>86</sup> ferrocene-containing polyallylamine,<sup>87</sup> poly(glycidyl methacrylate-*co*-vinylferrocene),<sup>88</sup> ferrocene-branched chitosan derivatives<sup>89</sup> etc.

The first generation of oxidase-based amperometric biosensors was based on the immobilization of oxidase enzymes on the surface of various electrodes. For these systems, the efficiency of electron transfer from the enzymes to the electrode has been found to be poor in the absence of a mediator. Taking the glucose biosensors as a model, the electron transfer between glucose oxidase (GOx) active sites and the electrode surface is the limiting factor in the performance of amperometric glucose biosensors. Because of the thick protein layer surrounding its flavin adenine dinucleotide (FAD) redox center as an inherent barrier, glucose oxidase does not directly transfer electrons to conventional electrodes.<sup>85</sup> In GOx biosensors employing organometallic redox mediators, the metal center shuttles electrons between the FAD center and the electrode surface, thus significantly improving the

performance of the sensors. The mediation cycle is shown in Figure 7, and the reactions involved are as follows (Scheme 2):



Scheme 2. Redox reactions in mediator-based glucose biosensors.<sup>85</sup>

$\text{M}_{(\text{ox})}$  and  $\text{M}_{(\text{red})}$  are the oxidized and reduced forms of the mediator, respectively. In this process two electrons are transferred from glucose to the redox centers of the GOx. These electrons then are transferred to the mediator, forming the reduced form of the mediator. The reduced form is re-oxidized at the electrode, giving a current signal proportional to the glucose concentration as the oxidized form of the mediator is regenerated.<sup>90</sup>

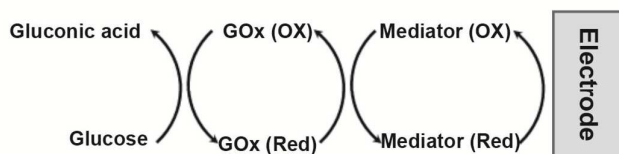


Figure 7. Sequence of events occurring in mediator-based glucose biosensors.<sup>85</sup> Reprinted with permission from *ref.* 85. Copyright (2008) American Chemical Society.

Hydrogel films were obtained by crosslinking the drop casted films of enzymes and organometallic polymers to improve the stability and performance of the related biosensors. New materials were developed, with the aim of tailoring the interaction between the redox polymer and the enzyme and optimize the electron transfer between them. Polymer flexibility or segmental mobility, degree of functional density and hydration properties would all have impact on the performance of the sensor.<sup>91</sup> For example, redox polymer hydrogel films with glucose oxidase were formed by photoinitiated free-radical polymerization of poly(ethylene glycol) and vinylferrocene with a film thickness of  $\sim 100 \mu\text{m}$ .<sup>90</sup> Electrodes decorated with a crosslinked thin film of ferrocene-bearing poly(ethyleneimine) (PEI) and

glucose oxidase hydrogel have also been utilized as glucose sensor.<sup>91-92</sup> Efforts to reduce the film thickness have been made, as this was believed to enhance the sensing ability. To this end, by using crosslinkable polymers, it was possible to generate polymer coatings with varying thickness. R uhe and co-workers described the synthesis of poly(dimethylacrylamide) polymers containing both electroactive ferrocene moieties and photoreactive benzophenone groups which reacted as crosslinker.<sup>93</sup> The ferrocene containing polymer was mixed with GOx and was deposited as a thin film on the electrode surface. The polymer layer was cross-linked and became firmly adhered to the electrode as a hydrogel thin film upon brief irradiation with UV light. Glucose-oxidizing electrodes with very high catalytic current responses were obtained.

In another study, a thermoresponsive poly(*N*-isopropylacrylamide) (PNIPAM)-ferrocene polymer was synthesized and attached to a cysteamine-modified gold electrode by a simple grafting to method, forming a thin hydrophilic organometallic polymer film (Figure 8).<sup>94</sup> The organometallic polymer acted as a covalently bound mediator. The flexible, brush-like redox polymer thin layers allowed an efficient interaction with the enzyme [soluble glucose dehydrogenase (sGDH)] and enabled electrical communication between the cofactor pyrroloquinoline quinone (PQQ) of sGDH in the presence of glucose. At elevated temperature, the polymer shrank and the brush-like structure disappeared. Thus, the electron transfer between the electrode and sGDH could be controlled.

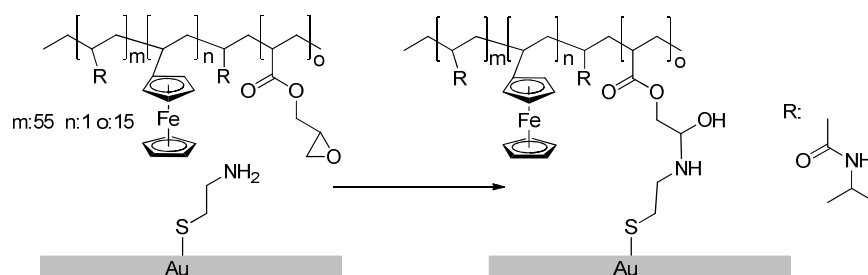


Figure 8. Fabrication of a covalently bound PNIPAM-ferrocene thin film on a gold electrode by a simple grafting to method.<sup>94</sup> Adapted with permission from *ref. 94*. Copyright (2007) American Chemical Society.

Polymer brushes containing ferrocene groups have been explored for decorating electrodes for electrochemical sensing. For example, Kang and co-workers developed an enzyme-mediated

amperometric biosensor on ITO electrodes via surface-initiated atom-transfer radical polymerization (ATRP) of ferrocenylmethyl methacrylate (FMMA) and glycidyl methacrylate (GMA) (Figure 9) under chemical control.<sup>95</sup> By ATRP, a ferrocene-containing organometallic polymer brush film was introduced on the electrode surface. Glucose oxidase was subsequently immobilized via coupling reactions to the glycidyl group in GMA segments. With the introduction of a redox-P(FMMA) block as the electron-transfer mediator, the enzyme-mediated ITO electrode exhibited high sensitivity.

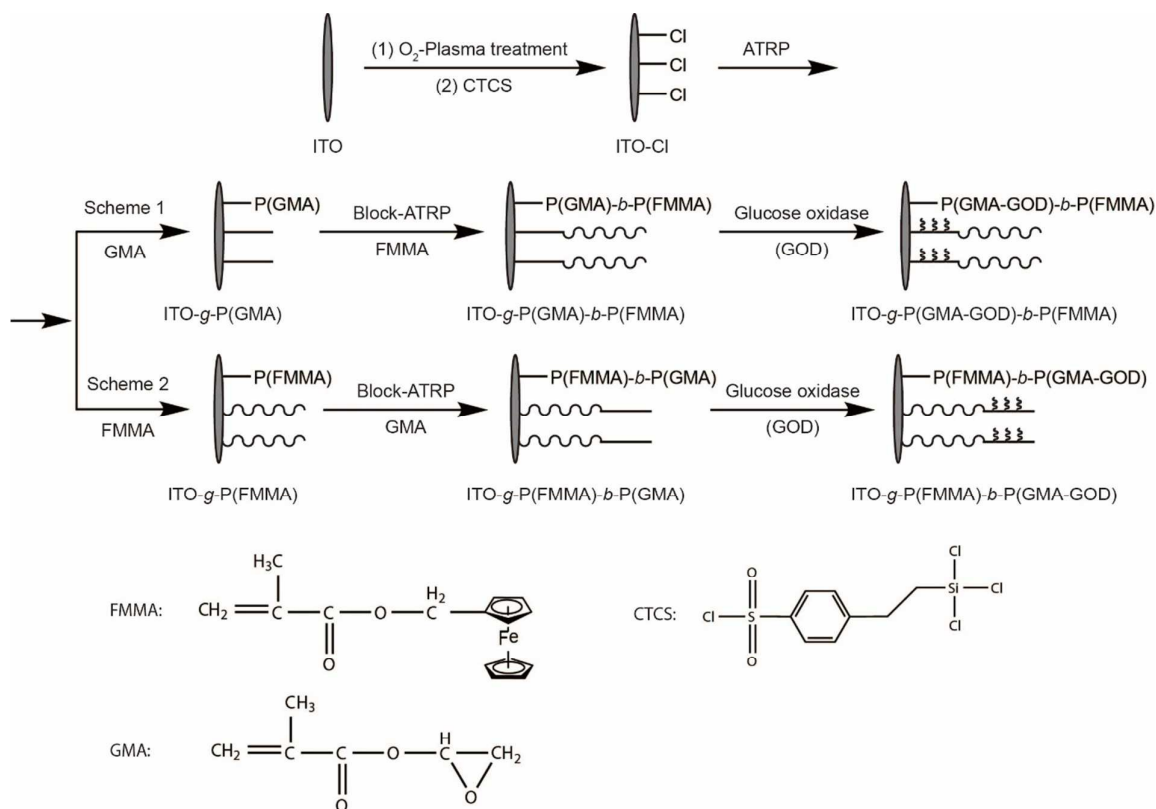


Figure 9. Ferrocene containing polymer brushes by SI-ATRP and the immobilization of Glucose oxidase on the thin film.<sup>95</sup> Adapted with permission from *ref. 95*. Copyright (2009) Elsevier.

In the above case, the ferrocene moieties of PFMMA segments in the polymer brush provide redox-active properties to the polymer while the GMA segments offer possible sites for coupling with functional groups, e.g. GOx. Liu et al. used the same organometallic polymer brushes obtained by consecutive SI-ATRP of FMMA and GMA as label-free electrochemical immunosensors for sensitive detection of tumor necrosis factor- $\alpha$  antigen (TNF- $\alpha$ ).<sup>96</sup> The redox-active ferrocene moieties in the

PFMMA segment were introduced on the Au electrode surface to generate redox responsive signals, while the abundant epoxy groups in PGMA segments offered various possibilities for coupling TNF- $\alpha$  antibodies by an aqueous carbodiimide coupling reaction. The antibody-coated electrode was used to detect target antigens by capturing TNF- $\alpha$  onto the electrode surface through immunoreactions, which would cause a drop of the redox currents of the film (Figure 10). The oxidation peak currents decreased linearly with TNF- $\alpha$  concentration in the range of 0.01 ng/ mL to 1  $\mu$ g/ mL with a detection limit of 3.94 pg/ mL. By monitoring the oxidation peak current of the electrode, an electrochemical biosensor for certain antigens with good sensitivity was realized.

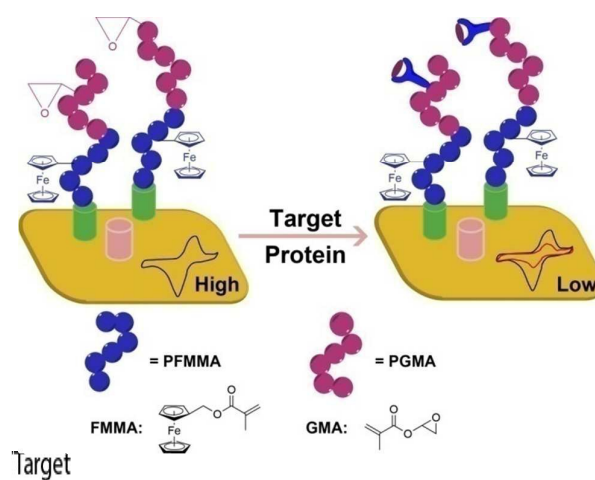


Figure 10. Label-free electrochemical immunosensors based on ferrocene-containing polymer brushes.<sup>96</sup> Adapted with permission from *ref. 96*. Copyright (2012) Elsevier.

Garrido and co-workers prepared poly(methacrylic acid) brushes on a diamond electrode which was dual-functionalized with the redox enzyme glucose oxidase and aminomethyl ferrocene. The authors demonstrated the amperometric detection of glucose by these organometallic polymer brushes.<sup>97</sup> The GOx and ferrocene moieties were well-distributed within the polymer brushes. This attempt offers an interesting strategy for the fabrication of smart electrodes for biosensors by electrical wiring of enzymes with a redox-responsive polymer.

A signal amplification strategy for electrochemical detection of DNA and proteins, based on ferrocene containing polymer brushes, was also reported.<sup>98</sup> The DNA capture probe (thiolated ssDNA) with a complementary sequence to the target DNA was immobilized on the electrode Au surface. After the

formation of sandwiched DNA duplexes with probe DNA, target DNA and the initiator-labeled detection probe DNA, poly(2-hydroxyethyl methacrylate) (PHEMA) brushes were grown from the duplexes in a controlled manner. The growth of long chain polymeric material provided abundant sites for subsequent coupling of electrochemically active ferrocene moieties. These ferrocene-containing polymers brushes in turn significantly enhanced the electrochemical signal output. The measured redox current of ferrocene was proportional to the logarithm of DNA concentration from 0.1 to 1000 nM.

The electrostatic layer-by-layer (LbL) assembly technique has been broadly employed as a simple and convenient approach in fabricating nanostructures with precise control of film structure and composition (in the film-surface normal direction).<sup>99-101</sup> The LbL assembly is usually based on the alternating adsorption of oppositely charged polyelectrolytes via electrostatic interaction. Furthermore, in addition to electrostatics, various other approaches for film assembly have been utilized to construct covalently bonded layers. For example, by covalent LbL assembly of periodate-oxidized glucose oxidase and the redox polymer poly(allylamine)ferrocene on cystamine modified Au electrode surfaces, highly stable glucose oxidase multilayer films were prepared as biosensing interfaces (Figure 11).<sup>102</sup> The electrode modified with the multilayer displayed excellent catalytic activity for the oxidation of glucose. The sensitivity of the sensor depended on the number of bilayers. The catalytic current with a certain glucose concentration was linearly related to the number of assembled layers. By controlling the number of bilayers on the Au electrode, the sensor sensitivity could be tuned.



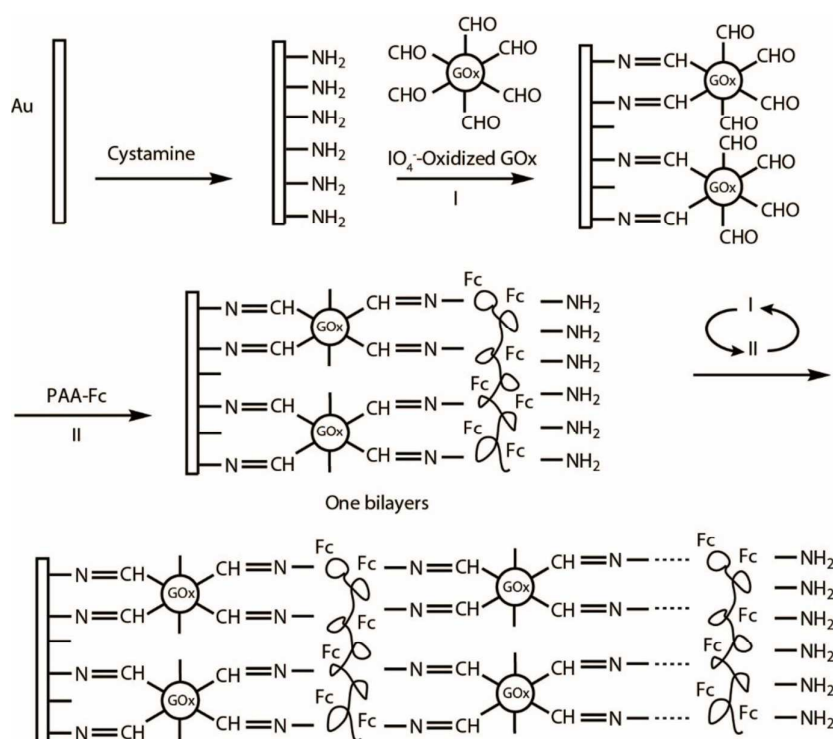


Figure 11. Layer-by-layer construction of GOx/PAA-Fc multilayer films on a Au electrode surface.<sup>102</sup> Reprinted with permission from *ref. 102*. Copyright (2004) Elsevier.

Electropolymerization is another suitable deposition approach for the formation of ferrocene-containing polymeric systems to obtain directly coupled layers at the electrode surface.<sup>26</sup> In this method, electropolymerizable monomers functionalized with ferrocene units were used, e.g. thiophene, pyrrole, aniline, or vinyl groups. Organometallic polymer films could be formed by this simple and reproducible process with controllable thickness and morphology. For example, Surinder et al. prepared a copolymer film of pyrrole and ferrocene carboxylate modified pyrrole (P(Py-FcPy)) on indium-tin-oxide (ITO) substrates by electrochemical polymerization. Glucose oxidase (GOx), the “model enzyme”, was entrapped during deposition in the fabrication of this electrochemical biosensor.<sup>103</sup> The redox properties of the pyrrole copolymer, enhanced by the presence of ferrocene moieties, showed a favorable electron transfer with an improved electrochemical signal for electrochemical biosensors. This example demonstrates the feasibility of fabricating sensitive electrochemical biosensors using ferrocene modified polypyrrole films.

### 3.1.2 Polymers containing ferrocene in the main chain

Redox responsive poly(ferrocenylsilane)s (PFSs) were also used to fabricate chemo/biosensors. PFSs<sup>4, 25</sup> belong to the class of organometallic polymers which are composed of alternating ferrocene and silane units in the main chain. These polymers can be reversibly oxidized and reduced by chemical or electrochemical means.<sup>104-106</sup> With the development of thermally induced, catalytic, living anionic and living photo-polymerization of silicon-bridged ferrocenophanes, well-defined PFSs showing a wide range of chain-substituted forms have become available.<sup>23, 107</sup> The processability and redox characteristics of PFSs make them suitable for the modification of surfaces and the fabrication of functional electrodes which have significant potential in the electrochemical detection of various analytes, including biological ones.

For example, our group fabricated various PFS grafts on electrodes through different approaches (simple “grafting to”, covalent layer-by-layer assembly and electrografting) and investigated the sensing abilities of these redox-active interfaces.

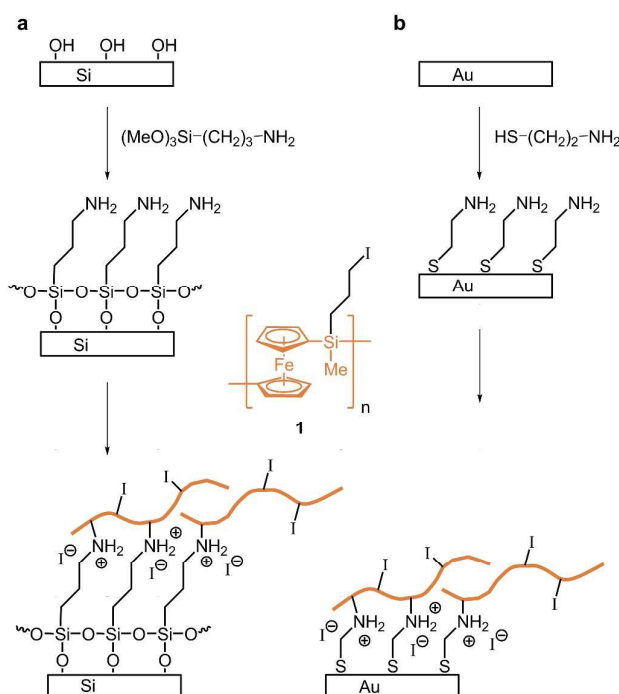


Figure 12. Schematic representation of the covalent surface-attachment of PFS chains (a) on a silicon substrate and (b) on a gold substrate. Reproduced from *ref. 108* with permission from The Royal Society of Chemistry.

Poly(ferrocenyl(3-iodopropyl)methylsilane) was covalently immobilized onto amine-modified surfaces by amination of iodopropyl side groups of PFS with a simple “grafting to” method, forming thin, uniform and relatively dense PFS films (Figure 12).<sup>108</sup> CV studies showed that the tethered PFS grafts on the electrode could effectively catalyze the oxidation of ascorbic acid which formed the basis for the use of PFS-decorated electrodes as electrochemical sensor.

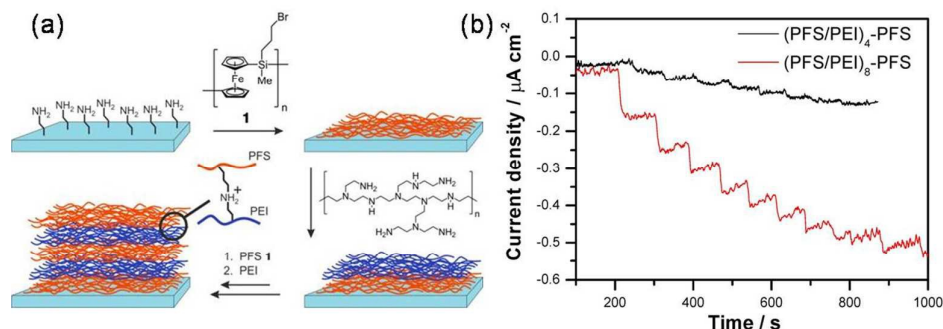


Figure 13. (a) Schematic representation of PFS/PEI multilayer fabrication on amine-functionalized substrates. (b) Amperometric response of (PFS/PEI)<sub>4</sub>-PFS and (PFS/PEI)<sub>8</sub>-PFS to H<sub>2</sub>O<sub>2</sub> at  $-0.1\text{V}$  (vs. Ag/AgCl) constant potential, where each step represents  $25\ \mu\text{M}$  H<sub>2</sub>O<sub>2</sub>. Adapted with permission from *ref. 109*. Copyright (2013) American Chemical Society.

This simple “grafting-to” method was extended further to include a covalent LbL deposition process. The sequential buildup of PFS layers was realized by using the amine alkylation reaction between PFS bromopropyl side groups and poly(ethylene imine) (Figure 13).<sup>109</sup> The thickness and composition of the grafts on the electrode could be precisely tuned. Owing to the formation of covalent bonds between the layers, these covalently interconnected layers do not disassemble upon oxidation and reduction, in contrast to PFS layers featuring similar backbones held together by electrostatic forces.<sup>15, 110-111</sup> PFS/PEI multilayers were successfully employed in the electrochemical sensing of ascorbic acid and hydrogen peroxide. In Figure 13b the sensor response of PFS multilayers with different number of bilayers is compared to consecutive additions of H<sub>2</sub>O<sub>2</sub>. Obviously, the amount of accessible ferrocene moieties per unit area at the electrode directly affects the performance of the sensor.

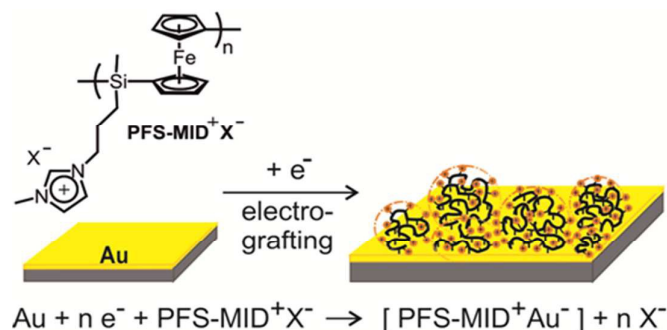


Figure 14. Electrografting of PFS on Au substrate in ionic liquid. Adapted with permission from *ref. 112*. Copyright (2014) American Chemical Society.

In another study by us, ultrathin, robust, dense, redox active organometallic PFS films were introduced to Au substrates using the electrografting method. The PFS grafts were formed within 5 min by cathodic reduction of Au substrates in a solution of imidazolium-functionalized PFS in the ionic liquid 1-ethyl-3-methylimidazolium ethyl sulfate (Figure 14).<sup>112</sup> The electrografting of the organometallic polymer followed the equation shown in Figure 14. The imidazolium side group of the PFS forms a complex with the auride ion ( $\text{Au}^-$ ) generated during the cathodic reduction of the Au substrate leading to the formation of new phases with the general formula  $[\text{PFS-MID}^+\text{Au}^-]$ . The Au electrodes were modified with PFS in this novel, simple and efficient method and employed as an ascorbic acid sensor. The amperometric response of the modified electrode to successive additions of ascorbic acid was evaluated at a fixed potential of 0.52 V (vs. Ag/AgCl), showing a rapid response and a high sensitivity.

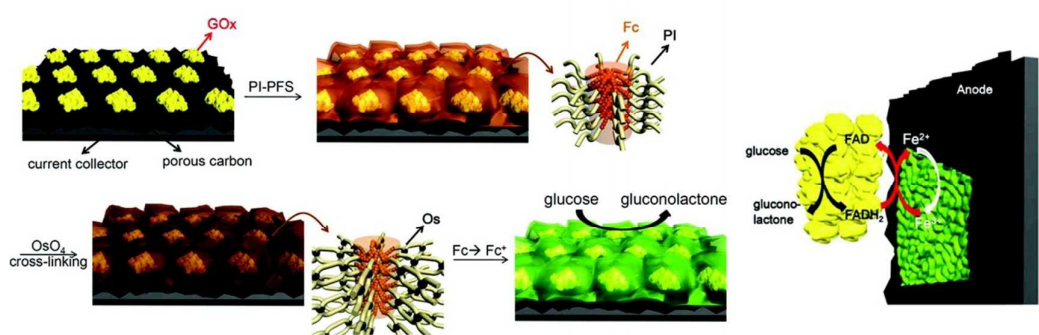


Figure 15. Fabrication process of electrodes comprised of GOx and PI-PFS mediators.<sup>113</sup> Adapted with permission from *ref. 113*. Copyright (2012) American Chemical Society.

A PFS based glucose sensor was fabricated by decorating porous carbon electrodes with a layer of glucose oxidase and by a film of polyisoprene-*b*-poly(ferrocenyldimethylsilane) (PI-*b*-PFDMS) by drop-coating followed by chemical crosslinking with OsO<sub>4</sub>.<sup>113</sup> It was found that the morphology of the film could be controlled by varying the block ratio of the copolymer and the composition of the casting solvent. By treatment with OsO<sub>4</sub>, a cross-linked and stable film was obtained. Glucose oxidase was employed as model enzyme and PI-*b*-PFDMS was used as electron mediator (Figure 15). The role of block copolymer morphology in the mediation of electron transport between the electrode and reaction center was investigated. The Fc moieties packed within the self-assembled structures were very useful to improve the electron transfer rate between the GOx and the electrode. The utilization of a biocontinuous microphase-separated block copolymer structure revealed a remarkable enhancement in catalytic currents and good glucose sensitivities at low glucose concentrations.

### ***3.1.3 Dendrimers containing ferrocene termini***

Dendrimers are well-defined, highly branched, star-shaped macromolecules bearing a large number of functional end groups at the periphery of the molecule. Metallo-dendrimers have been prepared and reported in the literature.<sup>114</sup> Dendrimers bearing ferrocene moieties belong to the family of redox-active organometallic polymers and are also useful in sensing applications. For example, redox active dendrimers consisting of flexible poly(propyleneimine) cores with octamethylferrocenyl units were deposited onto a platinum electrode and the system was applied as hydrogen peroxide and glucose sensor.<sup>115</sup> The dendrimer modified electrodes acted as electrocatalysts in the sensing application and the structural characteristics of the dendrimers influenced the sensor's behavior.

Astruc and co-workers synthesized a series of ferrocenyl dendrimers suitable for electrochemical sensing.<sup>116-121</sup> 1,2,3-Triazolylferrocenyl dendrimers prepared by click chemistry are selective electrochemical sensors for both transition-metal cations and oxo anions (H<sub>2</sub>PO<sub>4</sub><sup>-</sup> and ATP<sup>2-</sup>) with dramatic dendritic effects.<sup>118</sup> The ferrocenyl termini, which were directly attached to the triazole rings in the dendrimers, served as a redox monitor, showing a single, fully reversible CV wave (Figure 16).

When an oxo anion ( $\text{H}_2\text{PO}_4^-$  or  $\text{ATP}^{2-}$ , but not  $\text{HSO}_4^-$ ) or a transition-metal cation ( $\text{Cu}^+$ ,  $\text{Cu}^{2+}$ ,  $\text{Pd}^{2+}$ , or  $\text{Pt}^{2+}$ ) salt was added, the redox peak position of the ferrocenyl dendrimers shifted when they recognized certain oxo anions or transition metals. According to the Echegoyen-Kaifer model,<sup>122</sup> the process is a sign of a relatively “strong redox recognition”, indicated by only a shift of the initial CV wave.

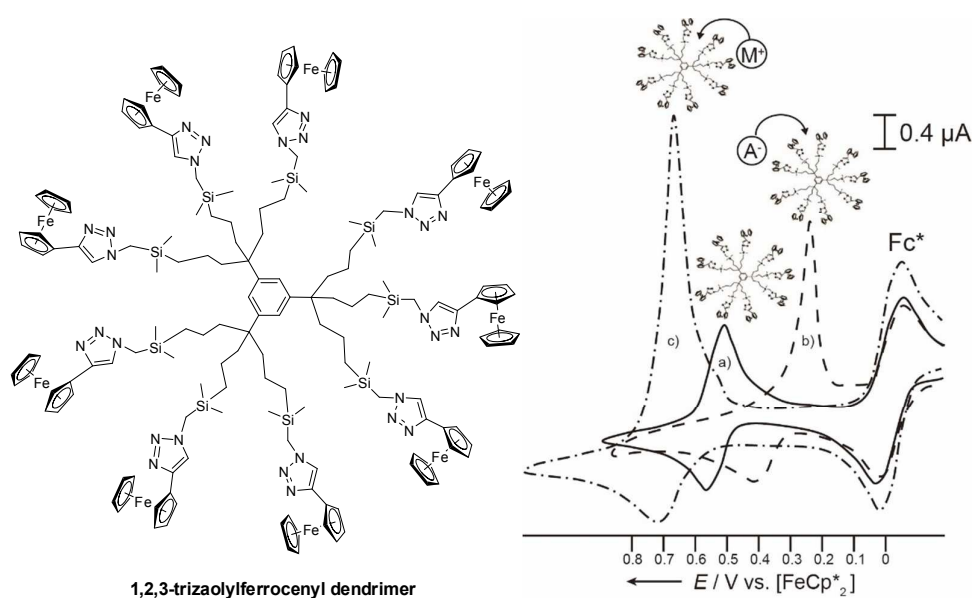


Figure 16. Structure of ferrocene-containing dendrimers and the redox sensing of both oxo anions ( $\text{A}^-$ ) and metal cations ( $\text{M}^+$ ) by poly-1,2,3-triazaolylferrocenyl dendrimers: cyclic voltammograms of dendrimers a) without and b) in the presence of  $(n\text{-Bu}_4\text{N})(\text{H}_2\text{PO}_4)$ ; c) in the presence of  $[\text{Pd}(\text{MeCN})_4](\text{BF}_4)_2$ .<sup>118</sup> Adapted with permission from *ref. 118*. Copyright (2007) Wiley-VCH.

For oxo anions, the peak position shifted to a less positive potential (Figure 16b), showing that the dendrimer-oxo anion assembly is easier to oxidize than the dendrimer itself. For metal cations, the oxidation peak appeared at a more positive potential (Figure 16c) than the initial peak, indicating that the cation-dendrimer assembly is more difficult to oxidize than the dendrimer. Thus the metallodendrimers containing ferrocene termini served as redox sensors for selective recognition of anions and cations.

### 3.2 Functionalization and applications with Os-containing compounds

Osmium is a transition metal in the platinum group and it can form compounds with oxidation states ranging from  $-2$  to  $+8$ . Os(II), Os(III) and Os(IV) complexes are the most widely used ones in

electrochemical studies.<sup>76</sup> Osmium-based redox organometallic polymers have attracted interest as efficient redox platforms for catalysis and biosensing because of their facile and reversible electron-transfer capability, and the possibility to tune the redox potential by changing the ligand and the backbone structure.<sup>123</sup> Figure 17 and Table 2 summarize the structures of several osmium-based polymers possessing redox centers distributed along the backbone,<sup>124</sup> such as poly(vinylimidazole) (PVI), poly(4-vinylpyridine) (P4VP), or polypyrrole and others<sup>125</sup> and their redox potential under certain conditions. Unlike the ferrocene moieties which are neutral groups within the polymer, Os complexes with ligands often introduce charges into the polymer.

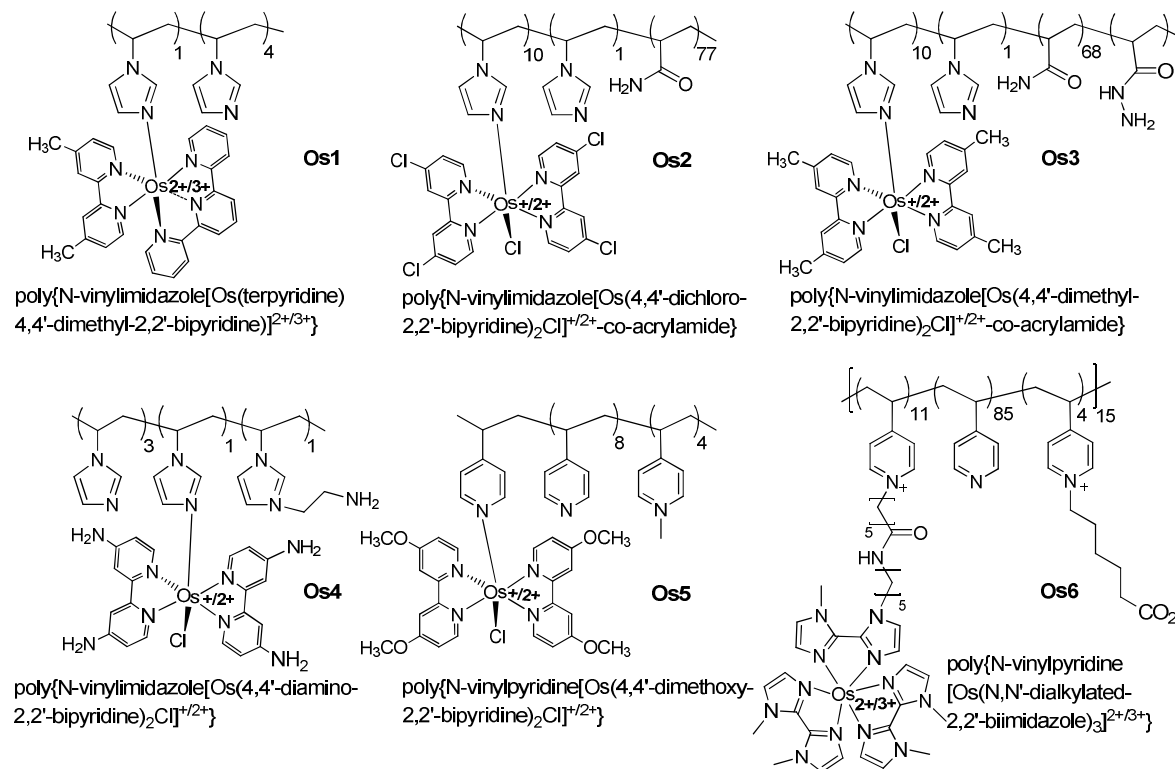


Figure 17. Molecular structures of osmium-based polymers **Os1** to **Os6**.<sup>124</sup>

Osmium-based polymers are excellent candidates as effective mediators for shuttling electrons between electrode and analytes and have been applied in biosensors for measuring ascorbic acid,<sup>126</sup> lactate,<sup>127</sup> H<sub>2</sub>O<sub>2</sub>,<sup>128</sup> dopamine,<sup>129</sup> etc.

There are many examples where osmium-containing organometallic polymers are used to "wire" enzymes in order to create amperometric biosensors. In enzyme electrodes, the polymer structure on the electrode is one of the key factors that influence the electron transfer rate, surface coverage of redox active centers, charge transport and propagation. Diffusion and permeation of soluble species through the polymer thus affect the performance of polymer-decorated electrodes in sensing.<sup>130</sup>

Table 2. Redox potential of osmium-based organometallic polymers.

<b>Compound</b>	<b>Redox potential (vs Ag/AgCl /V)</b>	<b>Ref.</b>	<b>Compound</b>	<b>Redox potential (vs Ag/AgCl / V)</b>	<b>Ref.</b>
<b>Os1</b>	+ 0.55, pH 5	<sup>131</sup>	<b>Os2</b>	+ 0.35, pH 7.4	<sup>132</sup>
<b>Os3</b>	+ 0.10, pH 5	<sup>133</sup>	<b>Os4</b>	- 0.16, pH 7.4	<sup>134</sup>
<b>Os5</b>	-0.069, pH 7.4	<sup>135</sup>	<b>Os6</b>	-0.19, pH 7.2	<sup>136</sup>

Like ferrocene-containing organometallic polymers, Os-containing polymers can also form stable hydrogels in aqueous solution and provide excellent matrices for immobilizing enzymes on electrode surfaces.<sup>137-139</sup> When enzymes and mediators are co-immobilized in the film, they are concentrated and closely connected which leads to strong bioelectrocatalytic activities. Much effort has been made to enhance the conductivity and performance of osmium-polymer-hydrogel-based biosensors.<sup>125, 140-144</sup> For example, new linkers have been introduced between the osmium complex and the polymer backbone,<sup>145</sup> co-electrodeposition techniques were employed to form crosslinked thin films from enzymes and polymers,<sup>146</sup> and carbon nanotubes or graphene were integrated with the polymers.<sup>147</sup>

Zafar et al. assembled FAD-dependent, glucose dehydrogenase (GcGDH) based hydrogel thin films with different Os polymers on graphite electrodes for glucose sensing.<sup>144</sup> Six different Os-containing polymers with PVI or P4VP backbone, whose redox potentials were tuned by the ligands, were employed in the immobilization of the enzyme. The type of Os-containing polymer and enzyme/Os polymer ratio significantly affect the performance of the biosensors.



A thermo-, pH-, and electrochemical-sensitive hydroxypropylcellulose-g-poly(4-vinylpyridine)-Os (bipyridine) (HPC-g-P4VP-Os (bpy)) graft copolymer (Figure 18) was synthesized by Huang et al.<sup>130</sup> A biosensor for glucose detection was fabricated by immobilizing GOx on the graft copolymer-decorated electrode. The water-soluble HPC backbone with excellent swelling ability provided an excellent environment for enzyme activity while the Os complex served as the redox mediator. The sensor showed an enhanced sensitivity for glucose detection up to 0.2 mM.

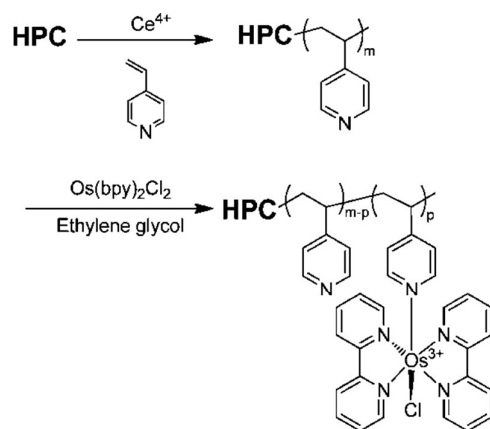


Figure 18. Preparation of HPC-g-P4VP-Os(bpy).<sup>130</sup> Adapted with permission from *ref. 130*. Copyright (2012) American Chemical Society.

Stable and porous films were formed by drop-coating electrodes with PVP-Os/chitosan and enzyme composites, showing an enhanced electrocatalytic activity for glucose sensing.<sup>58</sup> Porous structures (Figure 19B) resulted from random inter and intra polymeric cross-linking between two positively charged polymers, PVP-Os and chitosan by using glutaraldehyde, while the PVP-Os film had a homogeneous and smooth morphology (Figure 19A). When testing the GOx/PVP-Os- and GOx/PVP-Os/Chitosan- modified electrodes, the latter was found to exhibit a more than three times higher catalytic current. The enhanced catalytic conversion rate of the chitosan composite for glucose oxidation is a result of the stable incorporation of the enzyme into the porous and highly hydrophilic hydrogel. The porous structure enables the fast movement of chemicals involved in the glucose oxidation reaction.

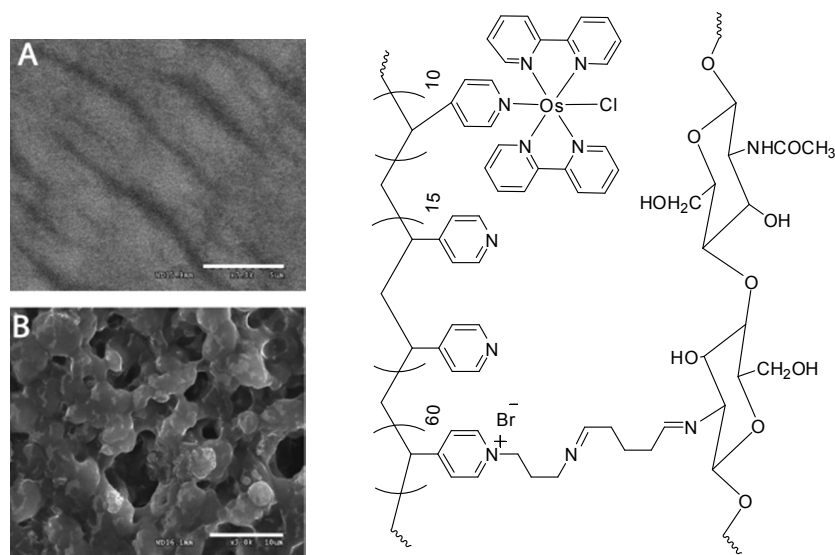


Figure 19. SEM images of the PVP-Os polymer (A) and PVP-Os/chitosan composite (B).<sup>58</sup> Adapted with permission from *ref.* 58. Copyright (2013) Wiley-VCH.

Zhang and Shen et al. also used the LbL assembly technique to modify the electrode with a polycation-bearing Os complex and glucose oxidase in the 1990s. The cyclic voltammetry curves they reported indicated that the osmium transferred the electrons successfully between the immobilized enzyme and the electrode surface.<sup>148</sup>

Minko, Katz et al. developed a smart sensing system based on an organometallic polymer containing Os centers in the side chains.<sup>149-150</sup> A poly(4-vinylpyridine) (P4VP) brush functionalized with Os(dmo-bpy)<sub>2</sub><sup>2+</sup> (dmo-bpy = 4,4'-dimethoxy-2,2'-bipyridine) redox groups was grafted to an ITO electrode. The electron exchange between the polymer-bound Os complex and the electrode was tuned by the swelling degree of the polymer chain. At pH < 4.5, due to the protonation of the pyridine groups, the film swelled, allowing electron exchange (Figure 20). At pH > 6, the polymer was in a collapsed state and the electrochemical process was inhibited because of frozen polymer chain motion.<sup>149</sup>

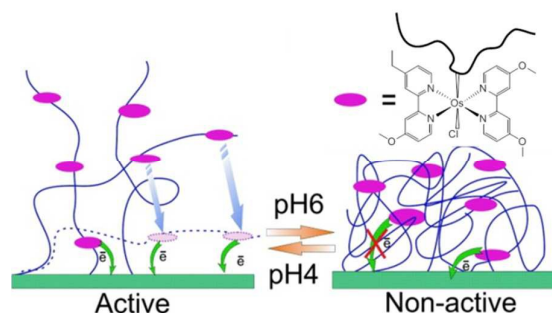


Figure 20. Reversible pH-controlled transformation of the Os-containing organometallic polymer on the electrode surface between electrochemically active and inactive states.<sup>150</sup> Adapted with permission from *ref. 150*. Copyright (2008) American Chemical Society.

The structural changes of the polymer enabled reversible transformations at the electrode surface between the active and the inactive states. The electrochemical activity of the Os-containing polymer modified electrode was combined with a biocatalytic reaction of glucose in the presence of soluble glucose oxidase (GOx), showing reversible activation of the bioelectrocatalytic process. The pH-controlled, switchable redox activity enabled the modified electrode to serve as a "smart" interface for a new generation of electrochemical biosensors with a signal controlled activity.<sup>150</sup>

Os-containing polymers also have potential uses in gene detection arrays.<sup>151-154</sup> For example, an Os-containing polymer in combination with the enzyme soybean peroxidase (SBP) was used to detect a single base pair mismatch in an 18-base oligonucleotide.<sup>151</sup> A single-stranded 18-base probe oligonucleotide was covalently attached to an Os-containing redox polymer film on a microelectrode, while the target single-stranded 18-base oligonucleotides were bound to the enzyme. Hybridization of the probe and target oligonucleotides (Figure 21) brought the enzyme close to the modified electrode which switched on the electrocatalytic reduction of  $\text{H}_2\text{O}_2$  to water. By monitoring the current enhancement, the single base mismatch in an oligonucleotide could be amperometrically sensed with the organometallic polymer-coated electrode.

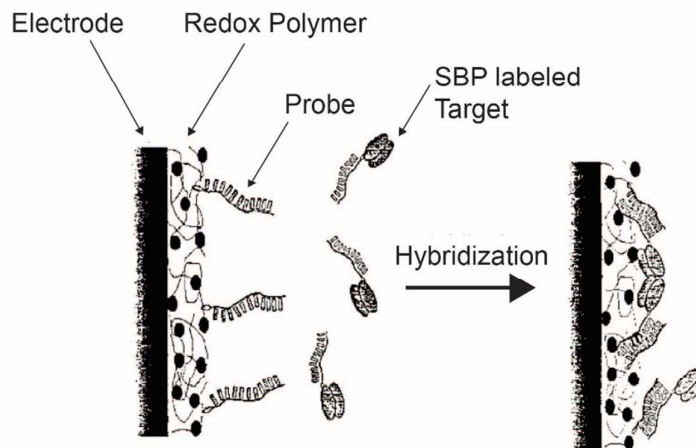


Figure 21. A DNA base-pair mismatch detection system based on an Os-containing polymer.<sup>151</sup> Reprinted with permission from *ref. 151*. Copyright (1999) American Chemical Society.

Employing a similar mechanism, an enzyme-amplified amperometric nucleic acid biosensor was proposed by Gao et al. based on sandwich-type assays.<sup>154</sup> Capture probe, sample DNA and detection probe with GOx formed a sandwich structure on the electrode by hybridization. The Os-containing organometallic polymer was introduced on the electrode surface by electrostatic interaction, activating and mediating the enzymatic reactions of the enzyme labels (Figure 22). With high electron mobility and good kinetics provided by the organometallic polymer, the nucleic acid molecules were amperometrically detected at femtomolar levels.

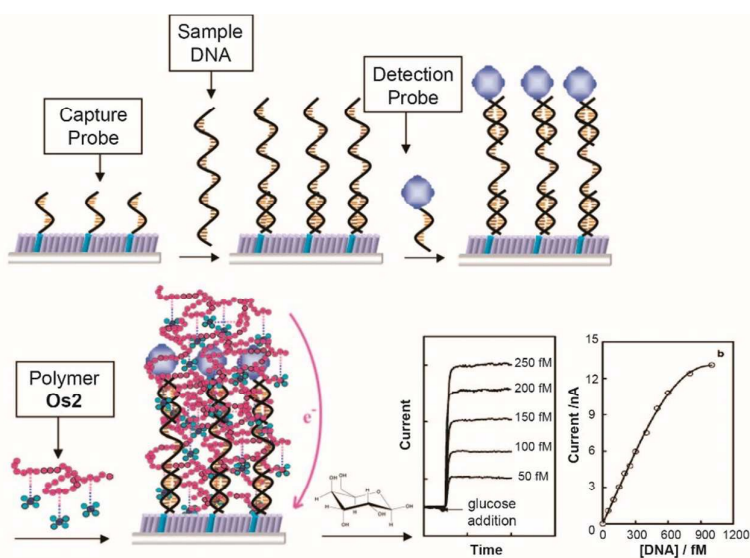


Figure 22. Illustration of the nucleic acid electrochemical activator bilayer detection platform.<sup>154</sup> Adapted with permission from *ref. 154*. Copyright (2004) American Chemical Society.

### 3.3 Immobilization and use of Co-containing molecules

Cobalt-based organometallic polymers are also well-suited for sensory applications as the coordination ability of the cobalt enables further bonding of specific analytes.<sup>155</sup> Compared to other metal centers, cobalt is less sensitive to water and oxygen in ambient conditions.<sup>156</sup> Swager et al. prepared a series of cobalt-containing conducting organometallic polymers and demonstrated that communication between the metal center and polymer backbone could be tuned by the reversible binding of small molecules. The energy levels of the metal-based orbitals could be altered which made these polymers highly suitable for small ligating molecules detection.<sup>34</sup>

For instance, a selective and effective detection system for the physiologically important species nitric oxide has been developed based on chemoresistive changes in a cobalt-containing conducting organometallic polymer film device.<sup>156</sup> The corresponding metal-containing monomer, featuring polymerizable 3,4-(ethylenedioxy)thiophene (EDOT) groups, was electropolymerized onto the working electrode surfaces, forming a conducting organometallic film (Figure 23A). The polymer film was highly conductive and the metal was intimately involved in the conduction pathway. When NO was exposed to the microelectrodes decorated with this cobalt-containing conducting polymer,

coordination of the ligand occurred, which changed the orbital energies of the complex, resulting in an increase in electrical resistance (Figure 23B). The cobalt metal center adopted a square pyramidal coordination arrangement to accommodate the addition of a bent NO ligand to form polymer-(NO) complexes. The device was insensitive to gases such as CO<sub>2</sub>, O<sub>2</sub> and CO while showing a large, irreversible resistance change when exposed to NO<sub>2</sub>.

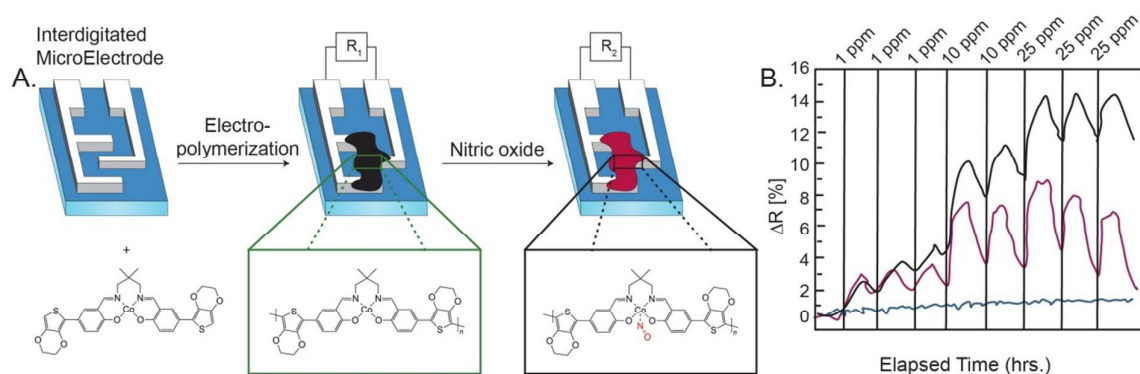


Figure 23. (A) Fabrication of conducting organometallic polymer electrode devices by electropolymerization across interdigitated microelectrodes (IME). (B) Chemoresistive response to NO gas exposure in dry N<sub>2</sub>. The unconditioned film is shown in black, the conditioned film at 0.262 V (vs Fc/Fc<sup>+</sup>) for 2 min is shown in red, and the poly-EDOT film is shown in blue.<sup>156</sup> Adapted with permission from *ref.* 156. Copyright (2006) American Chemical Society.

### 3.4 Electrode decoration with Ru-containing polymers

Organometallic polymers containing ruthenium are often used in photoelectrochemical sensors.<sup>157-160</sup>

The ruthenium moieties within the polymer serve as photoelectrochemically active materials. Take [Ru(bpy)<sub>3</sub>]<sup>2+</sup> (bpy=2,2'-bipyridine) as an example, where the excited state of Ru(II) is generated upon irradiation with light. The [Ru(bpy)<sub>3</sub>]<sup>2+</sup> can react as electron donor or acceptor, producing an anodic or cathodic photocurrent (Figure 24).<sup>161</sup>

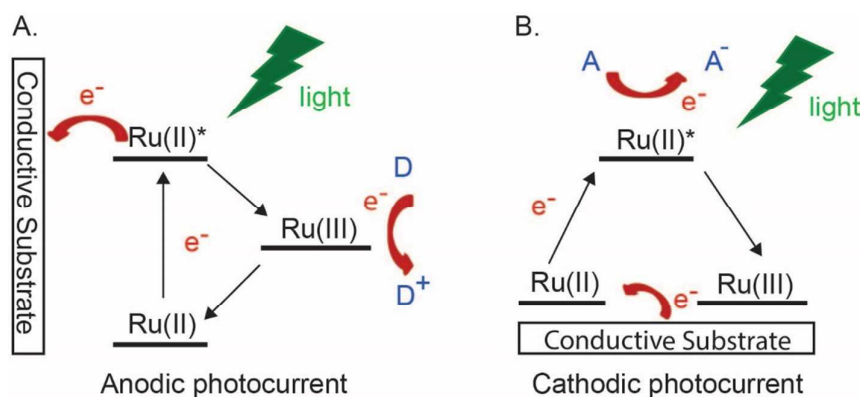


Figure 24. Schematic illustrations of A) anodic and B) cathodic photocurrent generation mechanisms by a ruthenium complex.<sup>161</sup> Adapted with permission from *ref. 161*. Copyright (2014) American Chemical Society.

Based on this phenomenon, Cosnier et al. fabricated several photoelectrochemical immunosensors for the detection of biologically important species.<sup>157</sup> For example, a biotinylated tri(bipyridyl) ruthenium(II) complex (Figure 25) with pyrrole groups was electropolymerized on the electrode to form a biotinylated Ru-containing polypyrrole film. A cathodic photocurrent could be generated under illumination in the presence of an oxidative quencher. The immunosensor platform was built by subsequently attaching avidin and biotinylated cholera toxin (the probe) to the Ru-containing organometallic polymer decorated electrode via the avidin-biotin reaction. The photocurrent of the layered system decreased as the increase in steric hindrance thwarted the diffusion of quencher molecules to the underlying Ru-containing polymer film. When the analyte, consisting of cholera toxin antibodies (anti-CT), was introduced to the system, the photocurrent further decreased, due to the specific binding of the antibodies to the electrode. By monitoring the variation of the photocurrent, detection of the corresponding antibody was realized from 0 to 200  $\mu\text{g/mL}$ .<sup>157</sup>

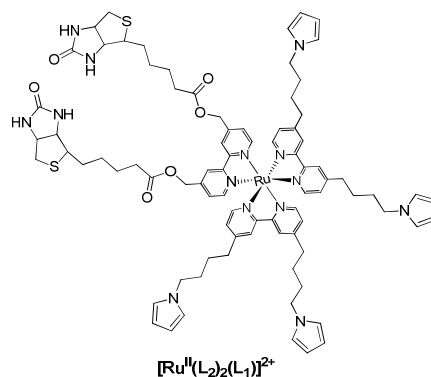


Figure 25. Structure of the biotinylated tri(bipyridyl) ruthenium(II) complex.<sup>157</sup>

Similarly, a label-free photoelectrochemical immunosensor and aptasensor were fabricated based on another Ru(II) containing organometallic copolymer. The bifunctional copolymer<sup>158</sup> was electropolymerized on the electrode using pyrenebutyric acid,  $N\alpha',N\alpha$ -bis(carboxymethyl)-L-lysine amide (NTA-pyrene) and [tris-(2,2'-bipyridine)(4,4'-(bis(4-pyrenyl-1-ylbutyloxy)-2,2'-bipyridine)] ruthenium (II) hexafluorophosphate (Ru(II)-pyrene complex). The pyrene groups, present in both compounds, underwent oxidative electropolymerization on platinum electrodes. The resulting copolymer contained NTA moieties, which functioned as an immobilization system for biotin- and histidine-tagged biomolecules, and Ru(II)-pyrene served as the photoelectrochemical transducing molecule.

Upon illumination, excited state of Ru(II) can be formed and further quenched by sacrificial electron donors or acceptors, generating photocurrent. For the construction of an immunosensor for cholera antitoxin antibodies (anti-CT) detection, biotin-Cu(NTA) interactions were used to modify the electrode with biotin-conjugated cholera toxin molecules (CT) (Figure 26A). The resulting copolymer-CT immunosensor was exposed to different anti-CT concentrations and the photocurrent responses were recorded. The normalized immunosensor response increased linearly with increasing antibody concentration (Figure 26B). By immobilizing thrombin binding aptamer (TBA) to the Ru-containing copolymer film, a photoelectrochemical aptasensor for thrombin was also developed (Figure 26 CD).



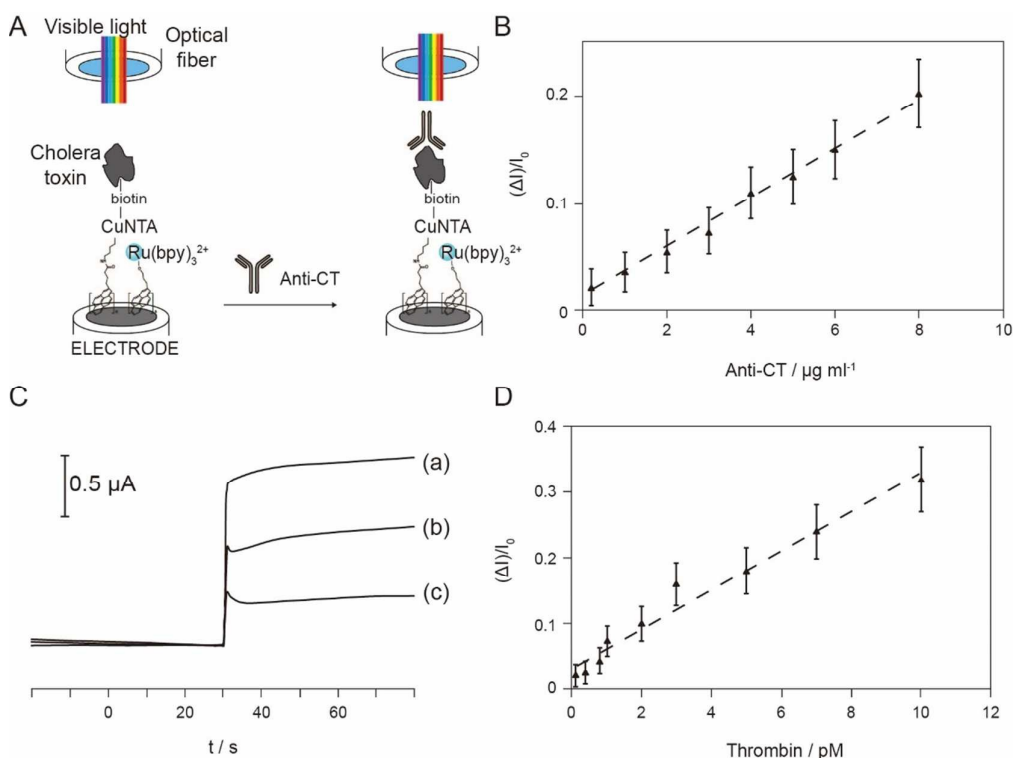


Figure 26. Photoelectrochemical immunosensor and aptasensor. A) Operating principle of the photoelectrochemical immunosensors. B) Calibration curve for sensing anti-CT concentrations ranging from 0 to 8  $\mu\text{g}/\text{mL}$ . C) Photocurrent measurement for the electrode a) before and b) after thrombin binding aptamer anchoring and c) after incubation with thrombin (12 pM) and D) calibration curve for photoelectrochemical aptasensing for thrombin concentrations ranging from 0 to 10 pM. All measurements were recorded in de-aerated 10 mM sodium ascorbate 0.1 M PBS solution.<sup>158</sup> Reprinted with permission from *ref.* 158. Copyright (2013) Elsevier.

### 3.5 Electrochemical sensors with metal-organic coordination polymers

Metal-organic coordination polymers (MOCP), also known as metal-organic frameworks (MOFs) or coordination networks utilize metal-ligand bonds to form polymer backbones. The wide range of choices for the organic linkers and metal ions for MOF construction have permitted the rational structural design of various MOFs with targeted properties.<sup>61, 162-164</sup> Ultrahigh porosity, large accessible surface areas, tunable structure, open metal sites, and high thermal and chemical stability of MOFs make them promising candidates for potential applications in many fields. Here we focus on the applications of MOFs in electrochemical sensing.

Some MOFs or MOF complexes exhibited excellent electrocatalytic activity, which is suitable for electrochemical sensor fabrication. For example, a two-dimensional Co-based metal-organic coordination polymer (Co-MOCP) was prepared by a simple solvothermal synthesis.<sup>165</sup> 1,3,5-Tri(1-imidazolyl)benzene, a typical imidazole-containing tripodal ligand with N donors, was used for the construction of the 2-D coordination architectures with  $\text{Co}^{2+}$ . The electrode decorated with Co-MOCP was used for the electrocatalytic oxidation of reduced glutathione (GSH).<sup>165</sup> This electrochemical sensor showed a wide linear range (from 2.5  $\mu\text{M}$  to 0.95 mM), low detection limit (2.5  $\mu\text{M}$ ), and high stability towards GSH, which renders it a good platform for GSH sensing.

Heterogeneous MOFs were also proposed for sensor fabrication. Hosseini et al. developed L-cysteine<sup>166</sup> and hydrazine<sup>167</sup> electrochemical sensors with Au-SH-SiO<sub>2</sub> nanoparticles immobilized on Cu-MOFs. Guo et al. demonstrated the electrocatalytic oxidation of NADH and reduction of H<sub>2</sub>O<sub>2</sub> with macroporous carbon (MPC) supported Cu-based MOF hybrids.<sup>168</sup>

Cu terephthalate MOFs were integrated with graphene oxide (GO) and deposited onto a glassy carbon electrode. The hybrid film was treated with electro-reduction to convert GO in the composite to graphene, the highly conductive reduced form.<sup>169</sup> Because of the synergistic effect from graphene's high conductivity and the unique electron mediating action of Cu-MOF, the decorated electrode showed a high sensitivity and low interference towards acetaminophen (ACOP) and dopamine (DA). By monitoring the oxidation peak current of the two drugs with differential pulse voltammetric (DPV) measurements, the concentrations of ACOP and DA could be determined.

Owing to high porosity and impressive absorption ability, MOFs could be used as novel and efficient immobilization matrices for enzymes. Glucose oxidase-based glucose biosensors and tyrosinase-based phenolic biosensors were fabricated with Au or Pt based organometallic polymers.<sup>170</sup> The coordinated organometallic polymer network can immobilize enzymes with high load/activity, showing improved mass-transfer efficiency, and the thus-prepared glucose and phenolic biosensors exhibited excellent performance with long-term stability. Figure 27 displays the one-pot fabrication process of the functional electrode and the biosensing mechanism. 2,5-Dimercapto-1,3,4-thiadiazole (DMcT) which

enables coordination of two or more metal ions was chosen to react with Au ions to form a porous structure in the presence of tyrosinase. Chronoamperometric measurements were used to monitor the current variation under different phenolic concentrations. The decorated electrode showed enhanced enzyme catalysis efficiency and excellent sensing performance towards phenol, resulting from the porous structure of the organometallic network which provided adequate space for enzyme entrapment and facilitated the mass transfer of the analytes and products.

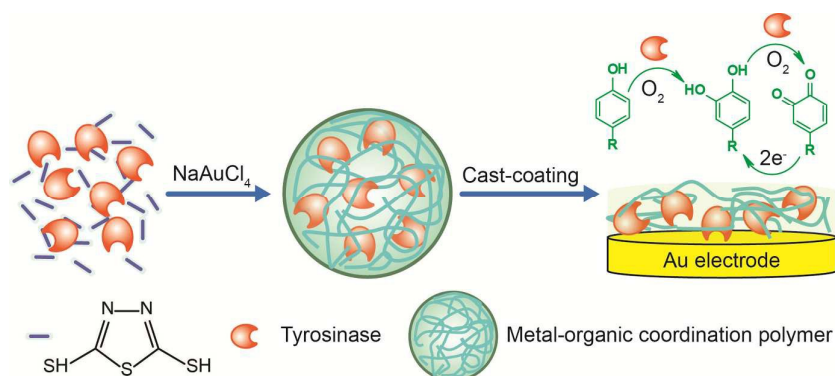


Figure 27. Illustration of the fabrication of tyrosinase-based phenolic biosensors and the biosensing mechanism.<sup>170</sup> Reprinted with permission from *ref.* 170. Copyright (2011) American Chemical Society.

Mao et al. studied a series of zeolitic imidazolate frameworks (ZIFs) as a matrix for integrated dehydrogenase-based electrochemical biosensors.<sup>171</sup> ZIFs with various pore sizes, surface areas and functional groups were investigated as matrix for co-immobilizing electrocatalysts (i.e., methylene green, MG) and dehydrogenases (i.e., glucose dehydrogenase, GDH). ZIF-70 [ $\text{Zn}(\text{Im})_{1.13}(\text{nIm})_{0.87}$ , Im=imidazole, nIm=2, nitroimidazole] showed outstanding adsorption capacities toward MG and GDH and was used to construct a biosensor by drop-casting MG/ZIF-70 on a glassy carbon electrode, followed by coating GDH onto the MG/ZIF-70 composite. In a continuous-flow system, the biosensor was linearly responsive to glucose in the range of 0.1 - 2 mM.

Electrochemical sensors for the differential pulse anodic stripping voltammetric determination of lead based on multi-wall carbon nanotubes@ $\text{Cu}_3(\text{BTC})_2$  (BTC=benzene-1,3,5-tricarboxylate)<sup>172</sup> and amino-functionalized  $\text{Cu}_3(\text{BTC})_2$ <sup>173</sup> were also reported. The sensing systems showed excellent calibration responses towards lead at low concentrations, resulting from the absorbing effect of the MOFs.

MOFs showed superior sorption properties towards small molecules. The high porosity and reversible sorption behavior suggests that the MOFs are suitable candidates for fabricating gas sensors. The absorption by, or desorption of molecules from the MOFs often induces changes in the dielectric properties of these materials.<sup>174</sup> By utilizing this characteristic, MOFs were applied as sensor materials for impedimetric gas sensors. For example, Achmann et al. constructed the first impedance sensor with Fe-1,3,5-benzenetricarboxylate-MOF (Fe-BTC) for humidity sensing, which responded linearly in the range of 0 to 2.5 vol% water.<sup>174</sup>

A rubidium ion containing metal-organic framework CD-MOF has been shown as a candidate for CO<sub>2</sub> detection. The organometallic polymer CD-MOF showed an extended cubic structure comprising units of six  $\gamma$ -cyclodextrins (CD), linked by rubidium ions, which could react with gaseous CO<sub>2</sub> to form CO<sub>2</sub>-bound CD-MOF. The absorption process is reversible (Figure 27). The pristine CD-MOF exhibited a high ionic conductivity. When binding with CO<sub>2</sub>, a large drop in the conductivity (~550-fold) was monitored by electrochemical impedance spectroscopy. The CO<sub>2</sub> sensors that were fabricated based on this principle were capable of measuring CO<sub>2</sub> concentrations quantitatively.<sup>175</sup> Figure 28 also shows the cyclic change of conductivity of the CD-MOF with sequential CO<sub>2</sub> absorption and desorption. The plot of average conductivity value vs. CO<sub>2</sub> concentration shows that the sensitivity of the conductivity change is relatively high at low CO<sub>2</sub> concentration. This example demonstrates that MOFs have a promising future in the field of quantitative sensing applications.

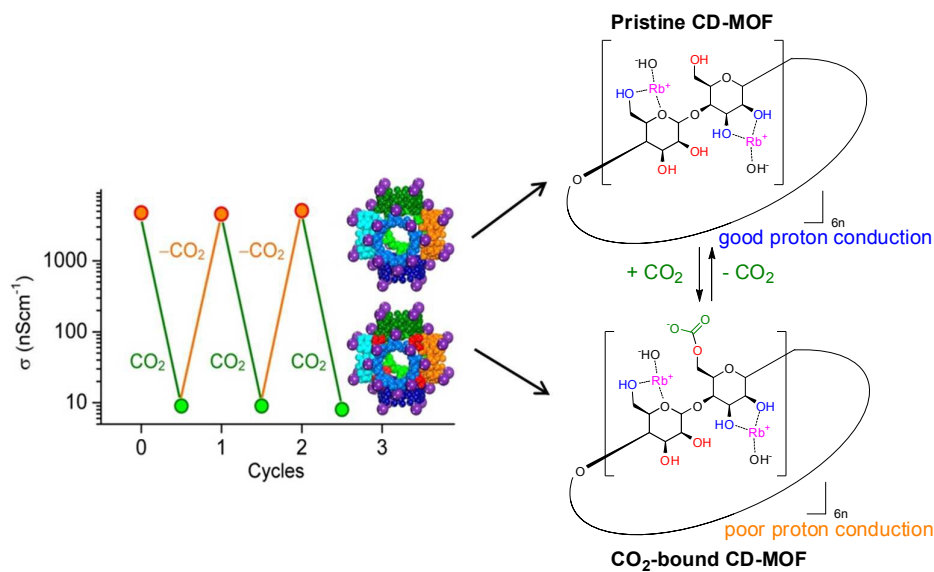


Figure 28: CO<sub>2</sub> sensor based on a Rubidium ion containing metal-organic framework CD-MOF.<sup>175</sup> Adapted with permission from *ref. 175*. Copyright (2014) American Chemical Society.

#### 4. Conclusions

This review summarizes the role of organometallic polymers as active components in electrochemical sensors. As illustrated, the presence of metal centers in the polymeric materials can introduce a variety of useful properties and render them a versatile and promising class of functional, soft materials. The resulting analytical performance of the chemo/biosensors relies intimately on the properties of the materials utilized to build the devices. Strategies of immobilization of organometallic polymers on electrode surfaces and opportunities for the resulting decorated electrodes in sensing are discussed. As is presented here, rational design of composition or structure of the organometallic components and improvements in fabrication techniques continuously advance the development of electrode surfaces towards greater sensing selectivity and lower limits of detection. Importantly, breakthroughs in the design and synthesis of organometallic polymers would open new avenues to further enhance performance and broaden the applicability and scope of electrochemical sensors.

The advente of nanotechnology techniques over the last decade has been promoting progress in the area of sensing applications, as well. In the future, efforts have to be made to integrate the advantages of nanotechnology and MEMS/microfluidic technology with the specific characteristics of

organometallic polymers for the development of fully automatic, label-free, highly sensitive, real-time chemo/biosensing. The MEMS/microfluidics devices, in particular, hold great promise for the fabrication of miniaturized, portable chemo/biosensors and biochips which, for example, may enable routine health checks at home, real-time environmental detection, etc. Such miniaturized and simplified devices also have great economic potential in the diagnostic market. Alternatively, employing the organometallic polymer to construct an array-based device that act as a chemical nose or be a constituent of other artificial organs, would also be attracting.

Taking the current knowledge to real-life applications is an important goal for the future. Organometallic polymers offer many exciting future opportunities and challenges in the electrochemical sensing and we hope that this review will assist to inspire future achievements and breakthroughs.

## 5. References

1. G. R. Whittell and I. Manners, *Adv. Mater.*, 2007, **19**, 3439-3468.
2. J. C. Eloi, L. Chabanne, G. R. Whittell and I. Manners, *Mater. Today*, 2008, **11**, 28-36.
3. J. W. Zhou, G. R. Whittell and I. Manners, *Macromolecules*, 2014, **47**, 3529-3543.
4. G. R. Whittell, M. D. Hager, U. S. Schubert and I. Manners, *Nat. Mater.*, 2011, **10**, 176-188.
5. I. Manners, *Science*, 2001, **294**, 1664-1666.
6. A. S. Abd-El-Aziz, C. Agatemor and N. Etkin, *Macromol. Rapid Commun.*, 2014, **35**, 513-559.
7. M. A. Vorotyntsev and S. V. Vasilyeva, *Adv. Colloid Interface Sci.*, 2008, **139**, 97-149.
8. A. S. Abd-El-Aziz, P. O. Shipman, B. N. Boden and W. S. McNeil, *Prog. Polym. Sci.*, 2010, **35**, 714-836.
9. S. J. Liu, Y. Chen, W. J. Xu, Q. Zhao and W. Huang, *Macromol. Rapid Commun.*, 2012, **33**, 461-480.
10. A. S. Abd-El-Aziz and E. A. Strohm, *Polymer*, 2012, **53**, 4879-4921.

11. I. Korczagin, R. G. H. Lammertink, M. A. Hempenius, S. Golze and G. J. Vancso, *Adv. Polym. Sci.*, 2006, **200**, 91-117.
12. X. Y. Ling, C. Acikgoz, I. Y. Phang, M. A. Hempenius, D. N. Reinhoudt, G. J. Vancso and J. Huskens, *Nanoscale*, 2010, **2**, 1455-1460.
13. R. A. Kruger and T. Baumgartner, *Dalton Trans.*, 2010, **39**, 5759-5767.
14. Z. R. Lin, *Adv. Mater.*, 1999, **11**, 1153-1154.
15. J. Song, D. Janczewski, Y. J. Ma, M. Hempenius, J. W. Xu and G. J. Vancso, *J. Mater. Chem. B*, 2013, **1**, 828-834.
16. S. Zou, I. Korczagin, M. A. Hempenius, H. Schonherr and G. J. Vancso, *Polymer*, 2006, **47**, 2483-2492.
17. J. J. McDowell, N. S. Zacharia, D. Puzzo, I. Manners and G. A. Ozin, *J. Am. Chem. Soc.*, 2010, **132**, 3236-3237.
18. C. L. Ho and W. Y. Wong, *Coord. Chem. Rev.*, 2013, **257**, 1614-1649.
19. D. Coquiere, J. Bos, J. Beld and G. Roelfes, *Angew. Chem. Int. Edit.*, 2009, **48**, 5159-5162.
20. F. S. Arimoto and A. C. Haven, *J. Am. Chem. Soc.*, 1955, **77**, 6295-6297.
21. J. B. Heilmann, M. Scheibitz, Y. Qin, A. Sundararaman, F. Jakle, T. Kretz, M. Bolte, H. W. Lerner, M. C. Holthausen and M. Wagner, *Angew. Chem. Int. Edit.*, 2006, **45**, 920-925.
22. T. Le Bouder, O. Maury, A. Bondon, K. Costuas, E. Amouyal, I. Ledoux, J. Zyss and H. Le Bozec, *J. Am. Chem. Soc.*, 2003, **125**, 12284-12299.
23. D. A. Foucher, B. Z. Tang and I. Manners, *J. Am. Chem. Soc.*, 1992, **114**, 6246-6248.
24. D. Foucher, R. Ziembinski, R. Petersen, J. Pudelski, M. Edwards, Y. Z. Ni, J. Massey, C. R. Jaeger, G. J. Vancso and I. Manners, *Macromolecules*, 1994, **27**, 3992-3999.
25. V. Bellas and M. Rehahn, *Angew. Chem. Int. Edit.*, 2007, **46**, 5082-5104.
26. C. Friebe, M. D. Hager, A. Winter and U. S. Schubert, *Adv. Mater.*, 2012, **24**, 332-345.
27. A. B. Powell, C. W. Bielawski and A. H. Cowley, *J. Am. Chem. Soc.*, 2010, **132**, 10184-10194.
28. P. R. Andres and U. S. Schubert, *Adv. Mater.*, 2004, **16**, 1043-1068.
29. A. S. Abd-El-Aziz and E. K. Todd, *Coord. Chem. Rev.*, 2003, **246**, 3-52.

30. U. S. Schubert and C. Eschbaumer, *Angew. Chem. Int. Edit.*, 2002, **41**, 2893-2926.
31. P. Nguyen, P. Gomez-Elipse and M. I, *Chem. Rev.*, 1999, **99**, 1515-1548.
32. C. Weder, *J. Inorg. Organomet. Polym. Mater.*, 2006, **16**, 101-113.
33. M. O. Wolf, *J. Inorg. Organomet. Polym. Mater.*, 2006, **16**, 189-199.
34. B. J. Holliday and T. M. Swager, *Chem. Commun.*, 2005, 23-36.
35. I. Manners, *Synthetic Metal-Containing Polymers*, wiley-VCH, Weinheim, 2004.
36. R. D. Archer, *Inorganic and Organometallic Polymers*, Wiley-VCH, Weinheim, 2001.
37. T. P. Russell, *Science*, 2002, **297**, 964-967.
38. M. A. C. Stuart, W. T. S. Huck, J. Genzer, M. Muller, C. Ober, M. Stamm, G. B. Sukhorukov, I. Szleifer, V. V. Tsukruk, M. Urban, F. Winnik, S. Zauscher, I. Luzinov and S. Minko, *Nat. Mater.*, 2010, **9**, 101-113.
39. L. Zhai, *Chem. Soc. Rev.*, 2013, **42**, 7148-7160.
40. M. E. A. Fegley, S. S. Pinnock, C. N. Malele and W. E. Jones, *Inorg. Chim. Acta*, 2012, **381**, 78-84.
41. N. J. Ronkainen, H. B. Halsall and W. R. Heineman, *Chem. Soc. Rev.*, 2010, **39**, 1747-1763.
42. L. E. Kreno, K. Leong, O. K. Farha, M. Allendorf, R. P. Van Duyne and J. T. Hupp, *Chem. Rev.*, 2012, **112**, 1105-1125.
43. L. M. Goldenberg, M. R. Bryce and M. C. Petty, *J. Mater. Chem.*, 1999, **9**, 1957-1974.
44. Y. Yang, G. A. Turnbull and I. D. W. Samuel, *Adv. Funct. Mater.*, 2010, **20**, 2093-2097.
45. D. Grieshaber, R. MacKenzie, J. Voros and E. Reimhult, *Sensors*, 2008, **8**, 1400-1458.
46. X. D. Wang and O. S. Wolfbeis, *Chem. Soc. Rev.*, 2014, **43**, 3666-3761.
47. Z. Wang, A. R. McWilliams, C. E. B. Evans, X. Lu, S. Chung, M. A. Winnik and I. Manners, *Adv. Funct. Mater.*, 2002, **12**, 415-419.
48. A. Wild, A. Winter, M. D. Hager and U. S. Schubert, *Analyst*, 2012, **137**, 2333-2337.
49. C. J. Qin, W. Y. Wong and L. X. Wang, *Macromolecules*, 2011, **44**, 483-489.



50. A. J. Lan, K. H. Li, H. H. Wu, D. H. Olson, T. J. Emge, W. Ki, M. C. Hong and J. Li, *Angew. Chem. Int. Edit.*, 2009, **48**, 2334-2338.
51. D. W. R. Balkenende, S. Coulibaly, S. Balog, Y. C. Simon, G. L. Fiore and C. Weder, *J. Am. Chem. Soc.*, 2014, **136**, 10493-10498.
52. C. Caliendo, E. Verona, A. Damico, A. Furlani, G. Infante and M. V. Russo, *Sens. Actuator B-Chem.*, 1995, **25**, 670-672.
53. C. Caliendo, I. Fratoddi, M. V. Russo and C. Lo Sterzo, *J. Appl. Phys.*, 2003, **93**, 10071-10077.
54. C. Caliendo, I. Fratoddi and M. V. Russo, *Appl. Phys. Lett.*, 2002, **80**, 4849-4851.
55. C. Caliendo, G. Contini, I. Fratoddi, S. Irrera, P. Pertici, G. Scavia and M. V. Russo, *Nanotechnology*, 2007, **18**.
56. P. Sun, Y. D. Jiang, G. Z. Xie, J. S. Yu, X. S. Du and J. Hu, *J. Appl. Polym. Sci.*, 2010, **116**, 562-567.
57. G. J. Zhou, W. Y. Wong, C. Ye and Z. Y. Lin, *Adv. Funct. Mater.*, 2007, **17**, 963-975.
58. H. D. Jirimali, R. K. Nagarale, J. M. Lee, D. Saravanakumar and W. Shin, *Chemphyschem*, 2013, **14**, 2232-2236.
59. P. Chadha and P. J. Ragogna, *Chem. Commun.*, 2011, **47**, 5301-5303.
60. S. J. Payne, G. L. Fiore, C. L. Fraser and J. N. Demas, *Anal. Chem.*, 2010, **82**, 917-921.
61. C. Wang, D. M. Liu and W. B. Lin, *J. Am. Chem. Soc.*, 2013, **135**, 13222-13234.
62. Y. L. Wang, L. Salmon, J. Ruiz and D. Astruc, *Nat. Commun.*, 2014, **5**, 3489.
63. M. H. Yan, S. K. P. Velu, G. Royal and P. Terech, *J. Colloid Interface Sci.*, 2013, **399**, 6-12.
64. B. R. Eggins, *Chemical sensors and biosensors*, John Wiley & Sons, West, Sussex, England, 2002.
65. A. Malinauskas, in *Encyclopedia of Surface and colloid science*, Marcel Dekker, New York, 2002, pp. 753-773.
66. J. M. Zen, A. S. Kumar and D. M. Tsai, *Electroanalysis*, 2003, **15**, 1073-1087.
67. J. L. Lutkenhaus and P. T. Hammond, *Soft Matter*, 2007, **3**, 804-816.
68. I. Tokarev, M. Motornov and S. Minko, *J. Mater. Chem.*, 2009, **19**, 6932-6948.

69. I. Tokarev and S. Minko, *Adv. Mater.*, 2009, **21**, 241-247.
70. I. Tokarev and S. Minko, *Soft Matter*, 2009, **5**, 511-524.
71. F. C. Krebs, *Sol. Energy Mater. Sol. Cells*, 2009, **93**, 394-412.
72. D. Belanger and J. Pinson, *Chem. Soc. Rev.*, 2011, **40**, 3995-4048.
73. G. Decher and J. B. Schlenoff, eds., *Multilayer Thin Films: Sequential Assembly of Nanocomposite Materials*, Wiley-VCH, Weinheim, 2012.
74. A. J. Bard and L. R. Faulkner, *Electrochemical Methods: Fundamentals and Applications.*, John Wiley & Sons, New York, 2nd edn., 2001.
75. T. J. Kealy and P. L. Pauson, *Nature*, 1951, **168**, 1039-1040.
76. A. L. Eckermann, D. J. Feld, J. A. Shaw and T. J. Meade, *Coord. Chem. Rev.*, 2010, **254**, 1769-1802.
77. A. Bondi, *Journal of Physical Chemistry*, 1964, **68**, 441-451.
78. Y. Ohashi, *Reactivity in Molecular Crystals*, Wiley-VCH, Hoboken, 2008.
79. W. A. Amer, L. Wang, A. M. Amin, L. A. Ma and H. J. Yu, *J. Inorg. Organomet. Polym. Mater.*, 2010, **20**, 605-615.
80. B. Fabre, *Accounts Chem. Res.*, 2010, **43**, 1509-1518.
81. K. L. Robinson and N. S. Lawrence, *Electroanalysis*, 2006, **18**, 677-683.
82. K. L. Robinson and N. S. Lawrence, *Anal. Chem.*, 2006, **78**, 2450-2455.
83. N. S. Lawrence and K. L. Robinson, *Talanta*, 2007, **74**, 365-369.
84. S. X. Zhang, Y. Q. Fu and C. Q. Sun, *Electroanalysis*, 2003, **15**, 739-746.
85. J. Wang, *Chem. Rev.*, 2008, **108**, 814-825.
86. T. Saito and M. Watanabe, *React. Funct. Polym.*, 1998, **37**, 263-269.
87. S. Koide and K. Yokoyama, *J. Electroanal. Chem.*, 1999, **468**, 193-201.
88. M. Senel, E. Cevik and M. F. Abasiyanik, *Sens. Actuator B-Chem.*, 2010, **145**, 444-450.
89. W. W. Yang, H. Zhou and C. Q. Sun, *Macromol. Rapid Commun.*, 2007, **28**, 265-270.

90. K. Sirkar and M. V. Pishko, *Anal. Chem.*, 1998, **70**, 2888-2894.
91. S. A. Merchant, D. T. Glatzhofer and D. W. Schmidtke, *Langmuir*, 2007, **23**, 11295-11302.
92. S. A. Merchant, T. O. Tran, M. T. Meredith, T. C. Cline, D. T. Glatzhofer and D. W. Schmidtke, *Langmuir*, 2009, **25**, 7736-7742.
93. C. Bunte, O. Prucker, T. Konig and J. Ruhe, *Langmuir*, 2010, **26**, 6019-6027.
94. B. Nagel, A. Warsinke and M. Katterle, *Langmuir*, 2007, **23**, 6807-6811.
95. Z. B. Zhang, S. J. Yuan, X. L. Zhu, K. G. Neoh and E. T. Kang, *Biosens. Bioelectron.*, 2010, **25**, 1102-1108.
96. L. Yuan, W. Wei and S. Q. Liu, *Biosens. Bioelectron.*, 2012, **38**, 79-85.
97. A. A. Reitinger, N. A. Hutter, A. Donner, M. Steenackers, O. A. Williams, M. Stutzmann, R. Jordan and J. A. Garrido, *Adv. Funct. Mater.*, 2013, **23**, 2979-2986.
98. Y. F. Wu, S. Q. Liu and L. He, *Anal. Chem.*, 2009, **81**, 7015-7021.
99. G. Decher, *Science*, 1997, **277**, 1232-1237.
100. Y. M. Yu, M. Z. Yin, K. Mullen and W. Knoll, *J. Mater. Chem.*, 2012, **22**, 7880-7886.
101. J. F. Quinn, A. P. R. Johnston, G. K. Such, A. N. Zelikin and F. Caruso, *Chem. Soc. Rev.*, 2007, **36**, 707-718.
102. S. X. Zhang, W. W. Yang, Y. M. Niu and C. Q. Sun, *Sens. Actuator B-Chem.*, 2004, **101**, 387-393.
103. N. Palomera, J. L. Vera, E. Melendez, J. E. Ramirez-Vick, M. S. Tomar, S. K. Arya and S. P. Singh, *J. Electroanal. Chem.*, 2011, **658**, 33-37.
104. Y. J. Ma, W. F. Dong, M. A. Hempenius, H. Mohwald and G. J. Vancso, *Nat. Mater.*, 2006, **5**, 724-729.
105. M. A. Hempenius, C. Cirimi, J. Song and G. J. Vancso, *Macromolecules*, 2009, **42**, 2324-2326.
106. X. F. Sui, L. van Ingen, M. A. Hempenius and G. J. Vancso, *Macromol. Rapid Commun.*, 2010, **31**, 2059-2063.
107. I. Manners, *Chem. Commun.*, 1999, 857-865.
108. X. F. Sui, X. L. Feng, J. Song, M. A. Hempenius and G. J. Vancso, *J. Mater. Chem.*, 2012, **22**, 11261-11267.

109. X. L. Feng, A. Curnurcu, X. F. Sui, J. Song, M. A. Hernpenius and G. J. Vancso, *Langmuir*, 2013, **29**, 7257-7265.
110. J. Song, D. Janczewski, Y. J. Ma, L. van Ingen, C. E. Sim, Q. L. Goh, J. W. Xu and G. J. Vancso, *Eur. Polym. J.*, 2013, **49**, 2477-2484.
111. J. Song, D. Janczewski, Y. J. Ma, M. Hempenius, J. W. Xu and G. J. Vancso, *J. Colloid Interface Sci.*, 2013, **405**, 256-261.
112. X. Feng, X. Sui, M. A. Hempenius and G. J. Vancso, *J. Am. Chem. Soc.*, 2014, **136**, 7865-7868.
113. J. Lee, H. Ahn, I. Choi, M. Boese and M. J. Park, *Macromolecules*, 2012, **45**, 3121-3128.
114. G. R. Newkome, E. F. He and C. N. Moorefield, *Chem. Rev.*, 1999, **99**, 1689-1746.
115. M. P. G. Armada, J. Losada, M. Zamora, B. Alonso, I. Cuadrado and C. M. Casado, *Bioelectrochemistry*, 2006, **69**, 65-73.
116. M. C. Daniel, F. Ba, J. R. Aranzaes and D. Astruc, *Inorg. Chem.*, 2004, **43**, 8649-8657.
117. D. Astruc, M. C. Daniel and J. Ruiz, *Chem. Commun.*, 2004, 2637-2649.
118. C. Ornelas, J. R. Aranzaes, E. Cloutet, S. Alves and D. Astruc, *Angew. Chem. Int. Edit.*, 2007, **46**, 872-877.
119. D. Astruc, C. Ornelas and J. R. Aranzaes, *J. Inorg. Organomet. Polym. Mater.*, 2008, **18**, 4-17.
120. J. Camponovo, J. Ruiz, E. Cloutet and D. Astruc, *Chem. -Eur. J.*, 2009, **15**, 2990-3002.
121. R. Djeda, A. Rapakousiou, L. Y. Liang, N. Guidolin, J. Ruiz and D. Astruc, *Angew. Chem. Int. Edit.*, 2010, **49**, 8152-8156.
122. S. R. Miller, D. A. Gustowski, Z. H. Chen, G. W. Gokel, L. Echegoyen and A. E. Kaifer, *Anal. Chem.*, 1988, **60**, 2021-2024.
123. D. A. Guschin, J. Castillo, N. Dimcheva and W. Schuhmann, *Anal. Bioanal. Chem.*, 2010, **398**, 1661-1673.
124. S. C. Barton, J. Gallaway and P. Atanassov, *Chem. Rev.*, 2004, **104**, 4867-4886.
125. P. O. Conghaile, S. Poller, D. MacAodha, W. Schuhmann and D. Leech, *Biosens. Bioelectron.*, 2013, **43**, 30-37.
126. N. Havens, P. Trihn, D. Kim, M. Luna, A. K. Wanekaya and A. Mugweru, *Electrochim. Acta*, 2010, **55**, 2186-2190.

127. A. A. J. Torriero, E. Salinas, F. Battaglini and J. Raba, *Anal. Chim. Acta.*, 2003, **498**, 155-163.
128. T. M. Park, *Anal. Lett.*, 1999, **32**, 287-298.
129. H. F. Cui, Y. H. Cui, Y. L. Sun, K. Zhang and W. D. Zhang, *Nanotechnology*, 2010, **21**.
130. H. L. Kang, R. G. Liu, H. F. Sun, J. M. Zhen, Q. M. Li and Y. Huang, *J. Phys. Chem. B*, 2012, **116**, 55-62.
131. S. C. Barton, H. H. Kim, G. Binyamin, Y. C. Zhang and A. Heller, *J. Am. Chem. Soc.*, 2001, **123**, 5802-5803.
132. N. Mano, H. H. Kim, Y. C. Zhang and A. Heller, *J. Am. Chem. Soc.*, 2002, **124**, 6480-6486.
133. T. Chen, S. C. Barton, G. Binyamin, Z. Q. Gao, Y. C. Zhang, H. H. Kim and A. Heller, *J. Am. Chem. Soc.*, 2001, **123**, 8630-8631.
134. H. H. Kim, N. Mano, X. C. Zhang and A. Heller, *J. Electrochem. Soc.*, 2003, **150**, A209-A213.
135. N. Mano and A. Heller, *J. Electrochem. Soc.*, 2003, **150**, A1136-A1138.
136. N. Mano, F. Mao and A. Heller, *J. Am. Chem. Soc.*, 2002, **124**, 12962-12963.
137. X. F. Sui, X. L. Feng, M. A. Hempenius and G. J. Vancso, *J. Mater. Chem. B*, 2013, **1**, 1658-1672.
138. E. Suraniti, S. Vives, S. Tsujimura and N. Mano, *J. Electrochem. Soc.*, 2013, **160**, G79-G82.
139. H. M. Liu, C. X. Liu, L. Y. Jiang, J. Liu, Q. D. Yang, Z. H. Guo and X. X. Cai, *Electroanalysis*, 2008, **20**, 170-177.
140. T. J. Ohara, R. Rajagopalan and A. Heller, *Anal. Chem.*, 1994, **66**, 2451-2457.
141. M. Vreeke, R. Maidan and A. Heller, *Anal. Chem.*, 1992, **64**, 3084-3090.
142. E. Baldini, V. C. Dall'Orto, C. Danilowicz, I. Rezzano and E. J. Calvo, *Electroanalysis*, 2002, **14**, 1157-1164.
143. A. Heller, *Curr Opin Chem Biol*, 2006, **10**, 664-672.
144. M. N. Zafar, X. J. Wang, C. Sygmund, R. Ludwig, D. Leech and L. Gorton, *Anal. Chem.*, 2012, **84**, 334-341.
145. F. Mao, N. Mano and A. Heller, *J. Am. Chem. Soc.*, 2003, **125**, 4951-4957.

146. Z. Q. Gao, G. Binyamin, H. H. Kim, S. C. Barton, Y. C. Zhang and A. Heller, *Angew. Chem. Int. Edit.*, 2002, **41**, 810-813.
147. P. P. Joshi, S. A. Merchant, Y. D. Wang and D. W. Schmidtke, *Anal. Chem.*, 2005, **77**, 3183-3188.
148. Y. P. Sun, J. Q. Sun, X. Zhang, C. Q. Sun, Y. Wang and J. C. Shen, *Thin Solid Films*, 1998, **327**, 730-733.
149. T. K. Tam, J. Zhou, M. Pita, M. Ornatska, S. Minko and E. Katz, *J. Am. Chem. Soc.*, 2008, **130**, 10888-10889.
150. T. K. Tam, M. Ornatska, M. Pita, S. Minko and E. Katz, *J. Phys. Chem. C*, 2008, **112**, 8438-8445.
151. D. J. Caruana and A. Heller, *J. Am. Chem. Soc.*, 1999, **121**, 769-774.
152. C. N. Campbell, D. Gal, N. Cristler, C. Banditrat and A. Heller, *Anal. Chem.*, 2002, **74**, 158-162.
153. Y. C. Zhang, H. H. Kim and A. Heller, *Anal. Chem.*, 2003, **75**, 3267-3269.
154. H. Xie, C. Y. Zhang and Z. Q. Gao, *Anal. Chem.*, 2004, **76**, 1611-1617.
155. T. Shioya and T. M. Swager, *Chem. Commun.*, 2002, 1364-1365.
156. B. J. Holliday, T. B. Stanford and T. M. Swager, *Chem. Mat.*, 2006, **18**, 5649-5651.
157. N. Haddour, J. Chauvin, C. Gondran and S. Cosnier, *J. Am. Chem. Soc.*, 2006, **128**, 9693-9698.
158. W. J. Yao, A. Le Goff, N. Spinelli, M. Holzinger, G. W. Diao, D. Shan, E. Defrancq and S. Cosnier, *Biosens. Bioelectron.*, 2013, **42**, 556-562.
159. A. Le Goff and S. Cosnier, *J. Mater. Chem.*, 2011, **21**, 3910-3915.
160. Y. J. Qu, X. L. Liu, X. W. Zheng and Z. H. Guo, *Anal. Sci.*, 2012, **28**, 571-576.
161. W. W. Zhao, J. J. Xu and H. Y. Chen, *Chem. Rev.*, 2014, **114**, 7421-7441.
162. Q. L. Zhu and Q. Xu, *Chem. Soc. Rev.*, 2014, **43**, 5468-5512.
163. A. U. Czaja, N. Trukhan and U. Muller, *Chem. Soc. Rev.*, 2009, **38**, 1284-1293.
164. J. P. Lei, R. C. Qian, P. H. Ling, L. Cui and H. X. Ju, *Trac-Trends Anal. Chem.*, 2014, **58**, 71-78.

165. B. Q. Yuan, R. C. Zhang, X. X. Jiao, J. Li, H. Z. Shi and D. J. Zhang, *Electrochem. Commun.*, 2014, **40**, 92-95.
166. H. Hosseini, H. Ahmar, A. Dehghani, A. Bagheri, A. Tadjarodi and A. R. Fakhari, *Biosens. Bioelectron.*, 2013, **42**, 426-429.
167. H. Hosseini, H. Ahmar, A. Dehghani, A. Bagheri, A. R. Fakhari and M. M. Amini, *Electrochim. Acta*, 2013, **88**, 301-309.
168. Y. F. Zhang, X. J. Bo, C. Luhana, H. Wang, M. Li and L. P. Guo, *Chem. Commun.*, 2013, **49**, 6885-6887.
169. X. Wang, Q. X. Wang, Q. H. Wang, F. Gao, Y. Z. Yang and H. X. Guo, *ACS Appl. Mater. Interfaces*, 2014, **6**, 11573-11580.
170. Y. C. Fu, P. H. Li, L. J. Bu, T. Wang, Q. J. Xie, J. H. Chen and S. Z. Yao, *Anal. Chem.*, 2011, **83**, 6511-6517.
171. W. J. Ma, Q. Jiang, P. Yu, L. F. Yang and L. Q. Mao, *Anal. Chem.*, 2013, **85**, 7550-7557.
172. Y. Wang, Y. C. Wu, J. Xie, H. L. Ge and X. Y. Hu, *Analyst*, 2013, **138**, 5113-5120.
173. Y. Wang, H. L. Ge, Y. C. Wu, G. Q. Ye, H. H. Chen and X. Y. Hu, *Talanta*, 2014, **129**, 100-105.
174. S. Achmann, G. Hagen, J. Kita, I. M. Malkowsky, C. Kiener and R. Moos, *Sensors*, 2009, **9**, 1574-1589.
175. J. J. Gassensmith, J. Y. Kim, J. M. Holcroft, O. K. Farha, J. F. Stoddart, J. T. Hupp and N. C. Jeong, *J. Am. Chem. Soc.*, 2014, **136**, 8277-8282.

# Organometallic polymers for electrode decoration in sensing applications

